TOPICAL REVIEW

The nucleon-nucleon interaction

R. Machleidt† and I. Slaus‡

† Department of Physics, University of Idaho, Moscow, Idaho 83844, U. S. A.
‡ Triangle Universities Nuclear Laboratory (TUNL), Duke Station, Durham, North Carolina 27706, U. S. A. and Rudjer Boskovic Institute, Zagreb, Croatia

Abstract. We review the major progress of the past decade concerning our understanding of the nucleon-nucleon interaction. The focus is on the low-energy region (below pion production threshold), but a brief outlook towards higher energies is also given. The items discussed include charge-dependence, the precise value of the πNN coupling constant, phase shift analysis and high-precision NN data and potentials. We also address the issue of a proper theory of nuclear forces. Finally, we summarize the essential open questions that future research should be devoted to.

Submitted to: *J. Phys. G: Nucl. Part. Phys.*

1. Introduction

The nuclear force has been at the heart of nuclear physics ever since the field was born in 1932 with the discovery of the neutron by Chadwick [1]. In fact, during the first few decades of nuclear physics, the term 'nuclear forces' was often used as synonymous for nuclear physics as a whole [2]. There are good reasons why the nuclear force plays such an outstanding role.

The interaction between two nucleons is basic for all of nuclear physics. The traditional goal of nuclear physics is to understand the properties of atomic nuclei in terms of the 'bare' interaction between pairs of nucleons. With the onset of quantum-chromodynamics (QCD), it became clear that the nucleon-nucleon (NN) interaction is not fundamental. Nevertheless, even today, in any first approach towards a nuclear structure problem, one assumes the nucleons to be elementary particles. The failure or success of this approach may then teach us something about the relevance of subnuclear degrees of freedom.

The NN interaction has been investigated by a large number of physicists all over the world for the past 70 years. It is the empirically best known piece of strong interactions; in fact, for no other sample of the strong force a comparable amount of experimental data has been accumulated.

The oldest attempt to explain the nature of the nuclear force is due to Yukawa [3]. According to his theory, massive bosons (mesons) mediate the interaction between two nucleons. This idea spawned the sister discipline of particle physics. Although, in the light of QCD, meson theory is not perceived as fundamental anymore, the meson exchange concept continues to represent the best working model for a quantitative nucleon-nucleon potential.

Historically, it turned out to be a formidable task to describe the nuclear force just phenomenologically, and it took a quarter century to come up with the first semi-quantitative model [4]—in 1957. Ever since, there has been substantial progress in experiment and theory of the nuclear force. Most basic questions were settled in the 1960's and 70's such that in recent years we could concentrate on the subtleties of this peculiar force.

In this topical review, we will report the chief progress of the past decade. The focus will be on the low-energy region (below pion production threshold). Summaries of earlier periods and a pedagogical introduction into the field can be found in references [5, 6]. In the 1990's, major issues concerning the NN interaction have been:

- charge-dependence,
- the precise value of the πNN coupling constant,
- improved phase shift analysis,
- high-precision NN data,
- high-precision NN potentials,
- QCD and the nuclear force,
- NN scattering at intermediate and high energies.

We will now review these topics one by one.

2. Charge dependence

By definition, *charge independence* is invariance under any rotation in isospin space. A violation of this symmetry is referred to as charge dependence or charge independence breaking (CIB). *Charge symmetry* is invariance under a rotation by 180^0 about the y-axis in isospin space if the positive z-direction is associated with the positive charge. The violation of this symmetry is known as charge symmetry breaking (CSB). Obviously, CSB is a special case of charge dependence.

CIB of the strong NN interaction means that, in the isospin $T = 1$ state, the proton-proton ($T_z = +1$), neutron-proton ($T_z = 0$), or neutron-neutron ($T_z = -1$) interactions are (slightly) different, after electromagnetic effects have been removed. CSB of the NN interaction refers to a difference between proton-proton (pp) and neutron-neutron (nn) interactions, only. The charge dependence of the NN interaction is subtle, but in the $^1S_0$ state it is well established. The observation of small charge-dependent effects in this state is possible because the scattering length of an almost bound state acts like a powerful magnifying glass on the interaction.

The current understanding is that—on a fundamental level—the charge dependence of nuclear forces is due to a difference between the up and down quark masses and electromagnetic interactions among the quarks. A consequence of this are mass differences between hadrons of the same isospin multiplet and meson mixing. Therefore, if CIB is calculated based upon hadronic models, the mass differences between hadrons of the same isospin multiplet, meson mixing, and irreducible meson-photon exchanges are considered as major causes. For reviews on charge dependence, see references [7, 8, 9]. We will now summarize recent developments (that are not contained in any of these reviews).

2.1. Charge symmetry breaking

2.1.1. Experiment. As discussed, the scattering lengths in the $^1S_0$ state for pp, np, and nn scattering (denoted by a_{pp}, a_{np}, and a_{nn}, respectively) are the best evidence for the charge-dependence of nuclear forces. While we have well-established values for a_{pp} and a_{np} since many decades, the neutron-neutron scattering length continues to be a tough problem. The basic reason for this is that, so far, we have not been able to conduct any direct measurements of a_{nn} using free neutron-neutron collisions [10]. All current values are extracted from multi-particle reactions the analyses of which are beset with large theoretical uncertainties. The processes that are believed to have the smallest uncertainties are

$$\mu^- + d \to \nu_\mu + n + n\,, \tag{1}$$
$$\pi^- + d \to \gamma + n + n\,, \tag{2}$$
$$n + d \quad \to p + n + n\,. \tag{3}$$

While, there are no data on the first reaction, the other two processes have been studied repeatedly. In 1998, a very carefull study of the π^- induced reaction was published [11] and, in 1999, a renewed thorough investigation of the neutron induced process was accomplished [12], yielding results that are in perfect agreement, namely,

$$D(\pi^-, n\gamma)n\ [11] : a_{nn} = -18.50 \pm 0.53\ \text{fm}, \tag{4}$$
$$D(n, nnp)\ [12] : \quad a_{nn} = -18.7 \pm 0.6\ \text{fm}, \tag{5}$$

which can be summarised by

$$a_{nn} = -18.6 \pm 0.4\text{fm}. \tag{6}$$

Correcting for the neutron-neutron magnetic interaction, the pure nuclear value is:

$$a^N_{nn} = -18.9 \pm 0.4\text{fm}. \tag{7}$$

This summarizes the status by the end of 1999. Unfortunately, this is not the happy end of the story that everybody had hoped for. To properly discuss the new (and old) problems, we will first provide more details concerning the two types of reactions for which experiments have been conducted.

Over the past 20 years, there have been three independent studies of the reaction $\pi^- + d \to \gamma + n + n$. In one case [13], only the γ spectrum was measured, while in the other two cases [14, 11], kinematically complete experiments were performed measuring the γ and a neutron in the final state. The results are:

$$\begin{aligned} a_{nn} &= -18.60 \pm 0.34\ (\text{stat.}) \pm 0.26\ (\text{syst.}) \pm 0.30\ (\text{theor.})\ \text{fm} \\ &= -18.60 \pm 0.52\ \text{fm}\ [13], \end{aligned} \tag{8}$$
$$\begin{aligned} a_{nn} &= -18.70 \pm 0.42\ (\text{stat.}) \pm 0.39\ (\text{syst.}) \pm 0.30\ (\text{theor.})\ \text{fm} \\ &= -18.70 \pm 0.65\ \text{fm}\ [14], \end{aligned} \tag{9}$$
$$\begin{aligned} a_{nn} &= -18.50 \pm 0.05\ (\text{stat.}) \pm 0.44\ (\text{syst.}) \pm 0.30\ (\text{theor.})\ \text{fm} \\ &= -18.50 \pm 0.53\ \text{fm}\ [11]. \end{aligned} \tag{10}$$

Owing to the high spatial resolution of the gamma ray detector in reference [11], it was possible to assess the systematic errors due to uncertainties in the modelling of the stopped pion distribution in the target and in target vertex reconstruction in the Monte Carlo simulation. Therefore, the systematic uncertainties of the kinematically complete studies are now much better understood, and a very high statistical accuracy

in reference [11] makes the experimental uncertainty comparable to the theoretical one in the extraction of a_{nn} from the reaction $\mathrm{D}(\pi^-, \gamma n)n$. The combined result from all three studies gives the new world average for the $\mathrm{D}(\pi^-, \gamma)nn$ reaction

$$\begin{aligned} a_{nn} = & -18.59 \pm 0.27 \text{ (exper.)} \pm 0.30 \text{ (theor.) fm} \\ = & -18.59 \pm 0.40 \text{ fm.} \end{aligned} \tag{11}$$

In summary, the reaction $\pi^- + d \to \gamma + n + n$ appears to be in good shape.

Unfortunately, we cannot say the same about the neutron-induced deuteron breakup process. Until the recent investigation by the TUNL group, Gonzalez-Trotter *et al.* [12], all studies of the reaction $n + d \to p + n + n$ gave for a_{nn} values that differed from that obtained from the $\mathrm{D}(\pi^-, \gamma n)n$ process. Theoretical uncertainties in extracting a_{nn} from the neutron-induced deuteron breakup are much larger, as we will explain now.

First, in reactions with more than two nucleons in the final state, three nucleon forces (3NF) modify the cross section. It was suggested [15] that the 3NF is the reason why a_{nn} extracted from the $\mathrm{D}(n, nnp)$ process differs from that obtained from the $\mathrm{D}(\pi^-, \gamma n)n$ reaction. The 3NF are a natural consequence of strong interactions. Therefore, 3NF do exist, but the question is how significant they are and, in particular, do they affect a specific configuration of the nd breakup wherefrom one extracts a_{nn}. There are several indications for possible 3NF effects in nuclear physics: ^{3}H binding energy, nuclear matter binding energy, ^{4}He binding energy and negative parity excited states, ^{3}He and ^{4}He one-body density distributions, binding energies and radii of some nuclei, ^{17}O magnetic moment form factor, nd capture, A_y in elastic nd scattering, and space star, final state interaction (FSI) and quasifree scattering (QFS) configurations in the nd breakup [7, 16, 17]; but none of them provided conclusive information on 3NF. It was possible to reconcile all values of a_{nn} extracted from the studies of the reaction $\mathrm{D}(n, nnp)$ in the energy domain of 10 to 50 MeV with those obtained from the $\mathrm{D}(\pi^-, \gamma n)n$ process using the Fujita-Miyazawa 3NF [7]. However, the reanalyses of these nd breakup processes [18] gave values that differed considerably from those quoted by the original authors. Though any reanalysis is clouded by the lack of all relevant information, the main reason is the fact that original analyses used simple S-wave separable NN potentials, while the re-analyses were done using the rigorous three body theory of Glöckle *et al* [16]. Obviously, the claimed theoretical uncertainties in the original papers were underestimated.

Second, the magnetic interaction modifies the value of the $^1S_0$ scattering length extracted from the neutron induced deuteron breakup. It was shown [19] that for the neutron-pickup configuration in the neutron-induced deuteron breakup leading to the nn FSI there is a magnetic interaction in the $^1S_0$ state which is repulsive thereby decreasing the absolute value of a_{nn}. Depending on the NN potential (hard core or soft core), impulse approximation estimates of the effect of the magnetic interaction in the pickup configuration changes a_{nn} from -18.5 fm to -17.2 or even -16.4 fm [19]. The correction for the knockout configuration has the opposite sign since it is dominated by the magnetic interaction between a neutron and a proton in the $^1S_0$ state. The situation is more complex for the neutron-proton FSI, since the np FSI occurs in the $^1S_0$ and $^3S_1$ states.

The determination of a_{nn} by Gonzales-Trotter *et al* [12] has two characteristic features: first, it uses the rigorous theory [16] including, in addition to several realistic NN potentials, also the Tucson-Melbourne 3NF, and second, it performs a high-accuracy comparison of neutron-neutron and neutron-proton FSI in the $^1S_0$ state by

measuring cross sections of the reaction D(n, nnp) for identical kinematic conditions (the angle of the two emitted nucleons interacting in the $^1S_0$ final state is 28 to 43 deg) at the incident neutron energy of 13 MeV. Therefore, the neutron-proton scattering length, a_{np}, becomes the standard for determining a_{nn}. By comparing the extracted value for a_{np} and its uncertainty, it was possible to set an upper limit of 0.2 ± 0.6 fm on any possible effects due to 3NF influencing the extracted value of a_{nn}. Of course, it is possible that the effect of the magnetic interaction discussed by Slobodrian *et al* [19] are negligible in the energy/angular region studied by Gonzalez-Trotter *et al* [12]. On the other hand, it should be stressed that the rigorous calculations by Glöckle *et al* [16] do not include the electromagnetic interaction, and that there are now many indications of the shortcomings of the Tucson-Melbourne 3NF.

In the year of 2000, a new study of the neutron-neutron FSI in the D(n, nnp) reaction at the incident neutron energy of 25.3 MeV was published by the neutron group at Bonn [20]. The data were analyzed using the rigorous theory [16]. The extracted value is,

$$a_{nn} = -16.27 \pm 0.4 \text{ fm}, \tag{12}$$

which is in drastic disagreement with the result of the TUNL group [12] published in 1999 and also with those obtained from the D$(\pi^-, \gamma n)n$ process.

While most of the previous kinematically complete studies of the reaction D(n, nnp) employ a thick, active deuterated target measuring the energy of the proton, and detecting two neutrons at nearly the same angle on the same side of the incident neutron, this recent measurement [20] uses a thin deuterium target and detects a neutron at $\Theta_n = -55.5$ deg and a proton at $\Theta_p = 41.15$ deg. The advantage of this geometry is the reduction of the strong cross talk between neutron detectors and the reduction in losses from neutron multiple scattering. This geometrical configuration has the added advantage that the locus contains *np* QFS besides *nn* FSI and, therefore, provides a built-in normalization. Indeed, normalizing the data to *np* QFS yields a very similar value:

$$a_{nn} = -16.06 \pm 0.35 \text{ fm}. \tag{13}$$

Neither the use of different NN potentials nor the inclusion of the Tucson-Melbourne 3NF in the rigorous calculation produces noticeably different results for a_{nn}. This geometry at this incident energy is the region where the 3NF effect of the Tucson-Melbourne potential is very small. The preliminary result by the Bonn group—using the same incident energy of 25.3 MeV—gave a good fit to the *np* FSI spectrum using $a_{np} = -24$ fm.

The disagreement between the two most recent studies, Gonzalez-Trotter *et al* (TUNL) [12] and Huhn *et al* (Bonn) [20], opens again the problem of how completely do we understand the interactions involved in the three nucleon problem, specifically the 3NF. It also suggests that additional experimental studies at different incident energies and at different angles might be useful in resolving the problem.

When we use for a_{nn} the value obtained from the D$(\pi^-, \gamma)nn$ studies [equation (11)], correct it for the magnetic moment interaction [equation (7)], and compare it to the corresponding *pp* value [8]:

$$a_{pp}^N = -17.3 \pm 0.4 \text{ fm}, \tag{14}$$

then charge-symmetry is broken by the following amount,

$$\Delta a_{CSB} \equiv a_{pp}^N - a_{nn}^N = 1.6 \pm 0.6 \text{ fm}. \tag{15}$$

Table 1. CSB differences of the $^1S_0$ effective range parameters caused by nucleon mass splitting. 2π denotes the sum of all 2π-contributions and $\pi\rho$ the sum of all $\pi\rho$-contributions. TBE (non-iterative two-boson-exchange) is the sum of 2π, $\pi\rho$, and $(\pi\sigma + \pi\omega)$.

	kin. en.	OBE	2π	$\pi\rho$	$\pi\sigma + \pi\omega$	TBE	Total	Empirical
Δa_{CSB} (fm)	0.246	0.013	2.888	–1.537	–0.034	1.316	1.575	1.6 ± 0.6 fm
Δr_{CSB} (fm)	0.004	0.001	0.055	–0.031	–0.001	0.023	0.028	0.10 ± 0.12 fm

Recommended values for the corresponding effective ranges are [8],

$$r_{nn}^N = 2.75 \pm 0.11 \text{ fm}, \tag{16}$$

$$r_{pp}^N = 2.85 \pm 0.04 \text{ fm}, \tag{17}$$

implying

$$\Delta r_{CSB} \equiv r_{pp}^N - r_{nn}^N = 0.10 \pm 0.12 \text{ fm}. \tag{18}$$

Traditionally, it was believed that the meson mixing explains essentially all CSB effects. The largest contribution came from $\rho - \omega$ mixing, and there was very meager knowledge of $\pi - \eta$ mixing. Recently, CSB was studied by the comparison of two charge-symmetric processes: $\mathrm{D}(\pi^+, \eta)pp$ and $\mathrm{D}(\pi^-, \eta)nn$ in the energy region of the η threshold. The result for the ratio of the two processes in this energy region is $R = d\sigma^+/d\sigma^- = 0.937 \pm 0.007$, after a phase space correction is made for the difference in the threshold energies of the two reactions [21]. The deviation of R from 1 is an indication of CSB which is mostly due to $\pi - \eta$ mixing. A phenomenological fully relativistic model, which is based on coupled channel Nπ–Nη amplitudes, takes into account different nn and pp FSI and explicitly includes $\pi - \eta$ mixing, was developed [22] and compared to the data yielding for the $\pi - \eta$ mixing angle the value of (1.5 ± 0.4) deg, consistent with the mixing angle determined from particle decays and isospin-forbidden processes as well as with several other theoretical predictions [21].

2.1.2. Theory. The difference between the masses of neutron and proton represents the most basic cause for CSB of the nuclear force. Therefore, it is important to have a very thorough accounting of this effect.

The most trivial consequence of nucleon mass splitting is a difference in the kinetic energies: for the heavier neutrons, the kinetic energy is smaller than for protons. This raises the magnitude of the nn scattering length by 0.25 fm as compared to pp.

Besides the above, nucleon mass splitting has an impact on all meson-exchange diagrams that contribute to the nuclear force. In 1998, the most comprehensive and thorough calculation of these CSB effects ever conducted has been published [23]. The investigation is based upon the Bonn Full Model for the NN interaction [24]. Here, we will summarize the results. For this we devide the total number of meson exchange diagrams that is involved in the nuclear force into several classes. Below, we report the results for each class.

(i) **One-boson-exchange** (OBE, figure 1) contributions mediated by $\pi^0(135)$, $\rho^0(770)$, $\omega(782)$, $a_0/\delta(980)$, and $\sigma'(550)$. In the Bonn Full Model [24], the σ' describes only the correlated 2π exchange in $\pi\pi - S$-wave (and not the uncorrelated 2π exchange since the latter is calculated explicitly, cf. figure 2). Charge-symmetry is broken by the fact that for pp scattering the proton mass is

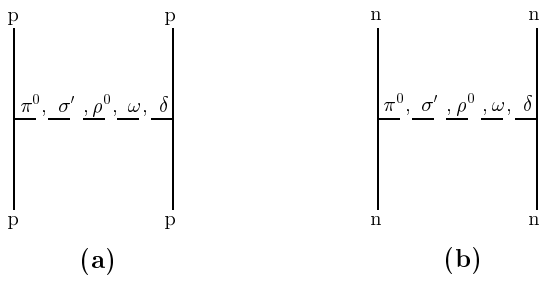

Figure 1. One-boson-exchange (OBE) contributions to (a) *pp* and (b) *nn* scattering.

used in the Dirac spinors representing the four external legs [figure 1(a)], while for *nn* scattering the neutron mass is applied [figure 1(b)]. The CSB effect from the OBE diagrams is very small (cf. table 1).

(ii) **2π-exchange diagrams.** This class consists of three groups; namely the diagrams with NN, NΔ and $\Delta\Delta$ intermediate states, where Δ refers to the baryon with spin and isospin $\frac{3}{2}$ and mass 1232 MeV. The most important group is the one with $N\Delta$ intermediate states which we show in figure 2. Part (a) of figure 2 applies to *pp* scattering, while part (b) refers to *nn* scattering. When charged-pion exchange is involved, the intermediate-state nucleon differs from that of the external legs. This is one of the sources for CSB from this group of diagrams. The 2π class of diagrams causes the largest CSB effect (cf. table 1 and dashed curve in figure 3).

(iii) **$\pi\rho$-exchanges.** Graphically, the $\pi\rho$ diagrams can be obtained by replacing in each 2π diagram (e. g., in figure 2) one pion by a ρ-meson of the same charge state. The effect is typically opposite to the one from 2π exchange.

(iv) **Further 3π and 4π contributions** ($\pi\sigma + \pi\omega$). The Bonn potential also includes some 3π-exchanges that can be approximated in terms of $\pi\sigma$ diagrams and 4π-exchanges of $\pi\omega$ type. The sum of the two groups is small, indicating convergence of the diagramatic expansion. The CSB effect from this class is essentially negligible.

The total CSB difference of the singlet scattering length caused by nucleon mass splitting amounts to 1.58 fm (cf. table 1) which agrees well with the empirical value 1.6 ± 0.6 fm. Thus, nucleon mass splitting alone can explain the entire empirical CSB of the singlet scattering length [25]. *This is a remarkable result.*

The impact of the various classes of diagrams on CSB phase shift differences are shown in figure 3. The total effect is the largest in the $^1S_0$ state where it is most noticable at low energy; e. g., at 1 MeV, the phase shift difference is 1.8 deg. The difference decreases with increasing energy and is about 0.15 deg at 300 MeV, in $^1S_0$.

The CSB effect on the phase shifts of higher partial waves is small; in P and D waves, typically in the order of 0.1 deg at 300 MeV and less at lower energies. This fact may suggest that CSB in partial waves other than $L = 0$ may be of no relevance.

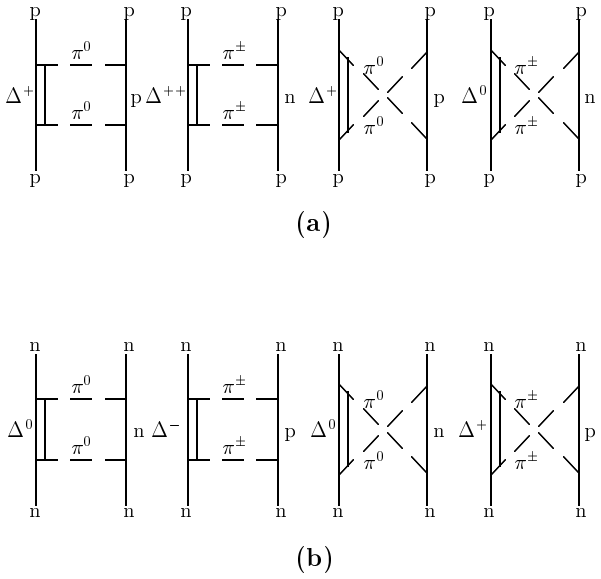

Figure 2. Two-pion-exchange contributions with $N\Delta$ intermediate states to (a) *pp* and (b) *nn* scattering.

In references [26] it was shown that this is not true: CSB beyond the S waves is crucial for the explanation of the Nolen-Schiffer anomaly.

Before finishing this subsection, a word is in place concerning other mechanisms that cause CSB of the nuclear force. Traditionally, it was believed that $\rho^0 - \omega$ mixing explains essentially all CSB in the nuclear force [8]. However, recently some doubt has been cast on this paradigm. Some researchers [27, 28, 29, 30] found that $\rho^0 - \omega$ exchange may have a substantial q^2 dependence such as to cause this contribution to nearly vanish in NN. Our finding that the empirically known CSB in the nuclear force can be explained solely from nucleon mass splitting (leaving essentially no room for additional CSB contributions from $\rho^0 - \omega$ mixing or other sources) fits well into this scenario. On the other hand, Miller [9] and Coon and coworkers [31] have advanced counter-arguments that would restore the traditional role of ρ-ω exchange. The issue is unresolved. Good summaries of the controversial points of view can be found in references [9, 32, 33].

Finally, for reasons of completeness, we mention that irreducible diagrams of π and γ exchange between two nucleons create a charge-dependent nuclear force. Recently, these contributions have been calculated to leading order in chiral perturbation theory [34]. It turns out that to this order the $\pi\gamma$ force is charge-symmetric (but does break charge independence).

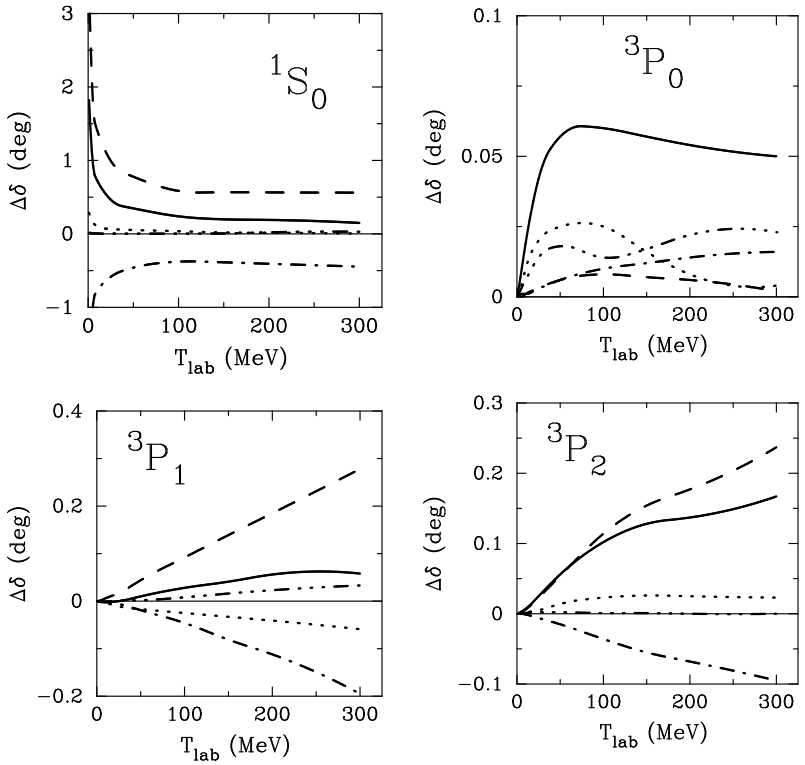

Figure 3. CSB phase shift differences $\delta_{nn} - \delta_{pp}$ (without electromagnetic interactions) for laboratory kinetic energies T_{lab} below 300 MeV and partial waves with $L \leq 1$. The CSB effects due to the kinetic energy, OBE, the entire 2π model, and $\pi\rho$ exchanges are shown by the dotted, dash-triple-dot, dashed, and dash-dot curves, respectively. The solid curve is the sum of all CSB effects.

2.2. Charge independence breaking

The empirical values for the *np* singlet effective range parameters are [35]:

$$a_{np} = -23.740 \pm 0.020 \text{ fm}, \quad r_{np} = 2.77 \pm 0.05 \text{ fm}. \tag{19}$$

It is useful to define the following averages:

$$\bar{a} \equiv \frac{1}{2}(a_{pp}^N + a_{nn}^N) = -18.1 \pm 0.6 \text{ fm}, \tag{20}$$

$$\bar{r} \equiv \frac{1}{2}(r_{pp}^N + r_{nn}^N) = 2.80 \pm 0.12 \text{ fm}. \tag{21}$$

Ignoring CSB, the CIB differences in the effective range parameters are given by:

$$\Delta a_{CIB} \equiv \bar{a} - a_{np} = 5.64 \pm 0.60 \text{ fm}, \tag{22}$$

$$\Delta r_{CIB} \equiv \bar{r} - r_{np} = 0.03 \pm 0.13 \text{ fm}. \tag{23}$$

The major cause of CIB in the NN interaction is pion mass splitting. Based upon the Bonn Full Model for the NN interaction [24], the CIB due to pion mass splitting

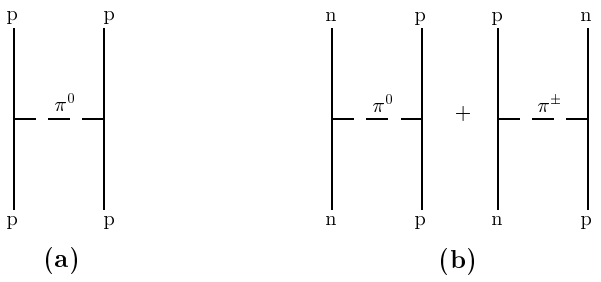

Figure 4. One-pion exchange (OPE) contributions to (a) *pp* and (b) *np* scattering.

has been calculated carefully and systematically in reference [36]. We will discuss now the various classes of diagrams and their contributions to CIB.

(i) **One-pion-exchange** (OPE). The CIB effect is created by replacing the diagram figure 4(a) by the two diagrams figure 4(b). The effect caused by this replacement can be understood as follows. In nonrelativistic approximation‡ and disregarding isospin factors, OPE is given by

$$V_{1\pi}(g_\pi, m_\pi) = -\frac{g_\pi^2}{4M^2}\frac{(\boldsymbol{\sigma}_1\cdot\mathbf{k})(\boldsymbol{\sigma}_2\cdot\mathbf{k})}{m_\pi^2+\mathbf{k}^2}\; F_{\pi NN}^2(\Lambda_{\pi NN}, |\mathbf{k}|) \qquad (24)$$

with M the average nucleon mass, m_π the pion mass, and $\mathbf{k}$ the momentum transfer. The above expression includes a πNN vertex form-factor, $F_{\pi NN}$, which depends on the cutoff mass $\Lambda_{\pi NN}$ and the magnitude of the momentum transfer $|\mathbf{k}|$. For $S=0$ and $T=1$, where S and T denote the total spin and isospin of the two-nucleon system, respectively, we have

$${}^{01}V_{1\pi}(g_\pi, m_\pi) = \frac{g_\pi^2}{m_\pi^2+\mathbf{k}^2}\;\frac{\mathbf{k}^2}{4M^2}\; F_{\pi NN}^2(\Lambda_{\pi NN}, |\mathbf{k}|)\,, \qquad (25)$$

where the superscripts 01 refer to ST. In the ${}^1S_0$ state, this potential expression is repulsive. The charge-dependent OPE is then,

$${}^{01}V_{1\pi}^{pp} = {}^{01}V_{1\pi}(g_{\pi^0}, m_{\pi^0}) \qquad (26)$$

‡ For pedagogical reasons, we use simple, approximate expressions to discuss the effects from pion exchange. Note, however, that in the calculations of reference [36] relativistic time-ordered perturbation theory is applied in its full complexity and without approximations.

Table 2. CIB contributions to the ${}^1S_0$ scattering length, Δa_{CIB}, and effective range, Δr_{CIB}, from various components of the NN interaction.

	OPE	2π	$\pi\rho$	$\pi\sigma+\pi\omega$	Total	Empirical
Δa_{CIB} (fm)	3.243	0.360	-0.383	1.426	4.646	5.64 ± 0.60
Δr_{CIB} (fm)	0.099	0.002	-0.006	0.020	0.115	0.03 ± 0.13

for *pp* scattering, and

$$ {}^{01}V_{1\pi}^{np} = 2\,{}^{01}V_{1\pi}(g_{\pi^\pm}, m_{\pi^\pm}) - {}^{01}V_{1\pi}(g_{\pi^0}, m_{\pi^0}) \tag{27} $$

for *np* scattering. If we assume charge-independence of g_π (i. e., $g_{\pi^0} = g_{\pi^\pm}$), then all CIB comes from the charge splitting of the pion mass, which is [37]

$$ m_{\pi^0} = 134.977 \text{ MeV}, \tag{28} $$

$$ m_{\pi^\pm} = 139.570 \text{ MeV}. \tag{29} $$

Since the pion mass appears in the denominator of OPE, the smaller π^0-mass exchanged in *pp* scattering generates a larger (repulsive) potential in the ${}^1S_0$ state as compared to *np* where also the heavier $\pi^\pm$-mass is involved. Moreover, the π^0-exchange in *np* scattering carries a negative sign, which further weakens the *np* OPE potential. The bottom line is that the *pp* potential is more repulsive than the *np* potential. The quantitative effect on Δa_{CIB} is such that it explains about 60% of the empirical value (cf. table 2). This has been know for a long time.

Due to the small mass of the pion, OPE is a sizable contribution in all partial waves including higher partial waves; and due to the pion's relatively large mass splitting (3.4%), OPE creates relatively large charge-dependent effects in all partial waves (see dashed curve in figure 5).

(ii) **2π-exchange diagrams.** We now turn to the CIB created by the 2π exchange contribution to the NN interaction. There are many diagrams that contribute (see reference [36] for a complete overview). For our qualitative discussion here, we pick the largest of all 2π diagrams, namely, the box diagrams with $N\Delta$ intermediate states, figure 6. Disregarding isospin factors and using some drastic approximation, the amplitude for such a diagram is

$$ V_{2\pi}(g_\pi, m_\pi) = -\frac{g_\pi^4}{16M^4}\frac{72}{25}\int \frac{d^3p}{(2\pi)^3}\frac{[\boldsymbol{\sigma}\cdot\mathbf{k}\boldsymbol{S}\cdot\mathbf{k}]^2}{(m_\pi^2+\mathbf{k}^2)^2(E_p+E_p^\Delta-2E_q)} \times F_{\pi NN}^2(\Lambda_{\pi NN}, |\mathbf{k}|)\, F_{\pi N\Delta}^2(\Lambda_{\pi N\Delta}, |\mathbf{k}|)\,, \tag{30} $$

where $\mathbf{k} = \mathbf{p} - \mathbf{q}$ with $\mathbf{q}$ the relative momentum in the initial and final state (for simplicity, we are considering a diagonal matrix element); $E_p = \sqrt{M^2+\mathbf{p}^2}$ and $E_p^\Delta = \sqrt{M_\Delta^2+\mathbf{p}^2}$ with $M_\Delta = 1232$ MeV the Δ-isobar mass; $\mathbf{S}$ is the spin transition operator between nucleon and Δ. For the $\pi N\Delta$ coupling constant, $f_{\pi N\Delta}$, the quark-model relationship $f_{\pi N\Delta}^2 = \frac{72}{25}f_{\pi NN}^2$ is used [24].

For small momentum transfers $\mathbf{k}$, this attractive contribution is roughly proportional to m_π^{-4}. Thus for the 2π exchange, the heavier pions will provide less attraction than the lighter ones. Charged and neutral pion exchanges occur for *pp* as well as for *np*, and it is important to take the isospin factors carried by the various diagrams into account. They are given in figure 6 below each diagram. For *pp* scattering, the diagram with double $\pi^\pm$ exchange carries the largest factor, while double $\pi^\pm$ exchange carries only a small relative weight in *np* scattering. Consequently, *pp* scattering is less attractive than *np* scattering which leads to an increase of Δa_{CIB} by 0.79 fm due to the diagrams of figure 6. The crossed diagrams of this type reduce this result and including all 2π exchange diagrams one finds a total effect of 0.36 fm [36].

(iii) **$\pi\rho$-exchanges.** This group is, in principle, as comprehensive as the 2π-exchanges discussed above. Graphically, the $\pi\rho$ diagrams can be obtained by replacing in

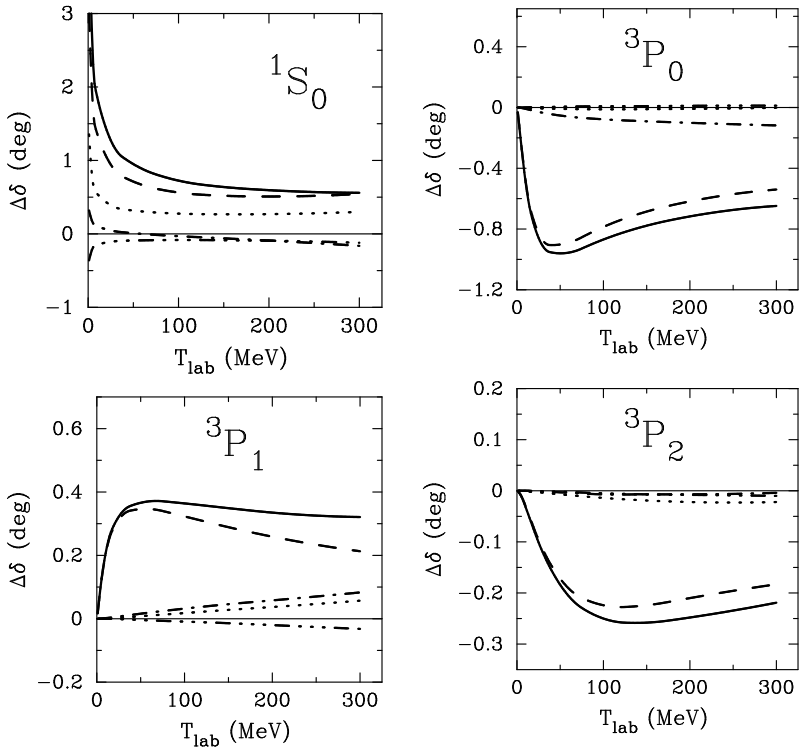

Figure 5. CIB phase shift differences $\delta_{np} - \bar{\delta}$ [with $\bar{\delta} \equiv (\delta_{pp} + \delta_{nn})/2$] for laboratory kinetic energies T_{lab} below 300 MeV and partial waves with orbital angular momentum $L \leq 1$. The CIB effects due to OPE, the entire 2π model, $\pi\rho$ exchanges, and $(\pi\sigma + \pi\omega)$ contributions are shown by the dashed, dash-dot, dash-triple-dot, and dotted curves, respectively. The solid curve is the sum of all CIB effects.

each 2π-diagram one of the two pions by a ρ-meson of the same charge-state. This contribution to CIB (dash-triple-dot curve in figure 5) is generally small, and (in most states) opposite to the one from 2π.

(iv) **Further 3π and 4π contributions** $(\pi\sigma + \pi\omega)$. As discussed, the Bonn potential also includes some 3π-exchanges that can be approximated in terms of $\pi\sigma$ diagrams and 4π-exchanges of $\pi\omega$ type. These diagrams carry the same isospin factors as OPE. The CIB effect from this class is very small, except in $^1S_0$ (dotted curve in figure 5). Notice that this effect has always the same sign as the effect from OPE (dashed curve), but it is substantially smaller. The reason for the OPE character of this contribution is that $\pi\sigma$ prevails over $\pi\omega$ and, thus, determines the character of this contribution. Since sigma-exchange is negative and since, futhermore, the propagator in between the π and the σ exchange is also negative, the overall sign of the $\pi\sigma$ exchange is the same as OPE. Thus, it is like a short-ranged OPE contribution.

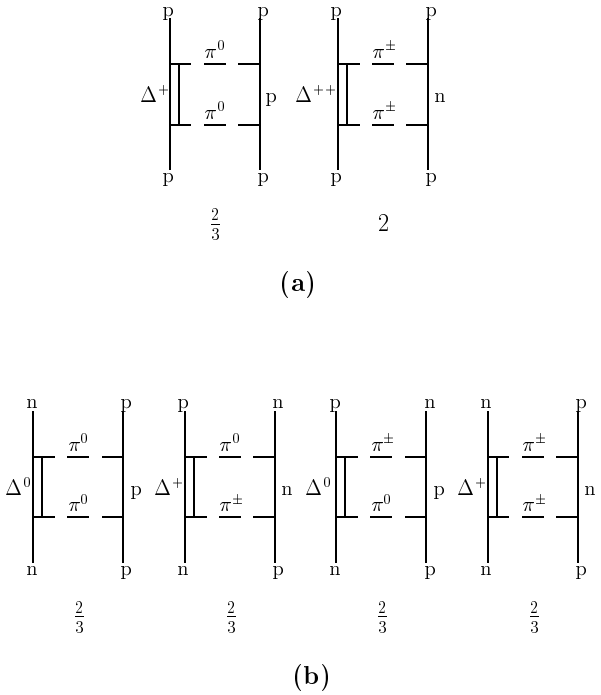

Figure 6. 2π-exchange box diagrams with $N\Delta$ intermediate states that contribute to (a) pp and (b) np scattering. The numbers below the diagrams are the isospin factors.

Concerning the singlet scattering length, the CIB contributions discussed explain about 80% of Δa_{CIB} (cf. table 2). Ericson and Miller [38] arrived at a very similar result using the meson-exchange model of Partovi and Lomon [39].

The sum of all CIB effects on phase shifts is shown by the solid curve in figure 5. Notice that the difference between the solid curve and the dashed curve (OPE) in that figure represents the sum of all effects beyond OPE. Thus, it is clearly seen that OPE dominates the CIB effect in all partial waves, even though there are substantial contributions besides OPE in some states, notably $^1S_0$ and $^3P_1$.

In reference [36], also the effect of rho-mass splitting on the $^1S_0$ effective range parameters was investigated. Unfortunately, the evidence for rho-mass splitting is very uncertain, with the Particle Data Group [37] reporting $m_{\rho^0} - m_{\rho^\pm} = 0.4 \pm 0.8$ MeV. Consistent with this, $m_{\rho^0} = 769$ MeV and $m_{\rho^\pm} = 768$ MeV, i. e., a splitting of 1 MeV was assumed, in the exploratory study of reference [36]. With this, one finds $\Delta a_{CIB} = -0.29$ fm from one-rho-exchange, and $\Delta a_{CIB} = 0.28$ fm from the non-iterative $\pi\rho$ diagrams with NN intermediate states. Thus, individual effects are small and, in addition, there are substantial cancellations between the two classes of diagrams that contribute. The net result is a vanishing effect. Thus, even if the rho-mass splitting will be better known one day, it will never be a great source of CIB.

Another CIB contribution to the nuclear force is irreducible pion-photon ($\pi\gamma$) exchange. Traditionally, it was believed that this contribution would take care of the remaining 20% of Δa_{CIB} [38, 40, 41]. However, a recently derived $\pi\gamma$ potential based

upon chiral perturbation theory [34] *decreases* Δa_{CIB} by about 0.5 fm, making the discrepancy even larger.

Thus, it is a matter of fact that about 25% of the charge-dependence of the singlet scattering length is not explained—at this time.

3. The πNN coupling constant

For the nuclear force, the pion is the most important meson. Therefore, it is crucial to have an accurate understanding of the coupling of the pion to the nucleon. In the 1990's, we have seen a controversial discussion about the precise value for the πNN coupling constant. We will first briefly review the events and then discuss in which way the NN data impose constraints on this important coupling constant.

From 1973 to 1987, there was a consensus that the πNN coupling constant is $g_\pi^2/4\pi = 14.3 \pm 0.2$ (equivalent to $f_\pi^2 = 0.079 \pm 0.001$§). This value was obtained by Bugg *et al.* [43] from the analysis of $\pi^\pm p$ data in 1973, and confirmed by Koch and Pietarinen [44] in 1980. Around that same time, the neutral-pion coupling constant was determined by Kroll [45] from the analysis of pp data by means of forward dispersion relations; he obtained $g_{\pi^0}^2/4\pi = 14.52 \pm 0.40$ (equivalent to $f_{\pi^0}^2 = 0.080 \pm 0.002$).

The picture changed in 1987, when the Nijmegen group [46] determined the neutral-pion coupling constant in a partial-wave analysis of pp data and obtained $g_{\pi^0}^2/4\pi = 13.1 \pm 0.1$. Including also the magnetic moment interaction between protons in the analysis, the value shifted to 13.55 ± 0.13 in 1990 [47]. Triggered by these events, Arndt *et al.* [48] reanalysed the $\pi^\pm p$ data to determine the charged-pion coupling constant and obtained $g_{\pi^\pm}^2/4\pi = 13.31 \pm 0.27$. In subsequent work, the Nijmegen group also analysed np, $\bar{p}p$, and πN data [49]. The status of their work as of 1993 is summarized in Ref. [50] where they claim that the most accurate values are obtained in their combined pp and np analysis yielding $g_{\pi^0}^2/4\pi = 13.47 \pm 0.11$ (equivalent to $f_{\pi^0}^2 = 0.0745 \pm 0.0006$) and $g_{\pi^\pm}^2/4\pi = 13.54 \pm 0.05$ (equivalent to $f_{\pi^\pm}^2 = 0.0748 \pm 0.0003$). The latest analysis of all $\pi^\pm p$ data below 2.1 GeV conducted by the VPI group using fixed-t and forward dispersion relation constraints has generated $g_{\pi^\pm}^2/4\pi = 13.75 \pm 0.15$ [51]. The VPI NN analysis extracted $g_{\pi^0}^2/4\pi \approx 13.3$ and $g_{\pi^\pm}^2/4\pi \approx 13.9$ as well as the charge-independent value $g_\pi^2/4\pi \approx 13.7$ [52, 53].

Also Bugg and coworkers have performed new determinations of the πNN coupling constant. Based upon precise $\pi^\pm p$ data in the 100–310 MeV range and applying fixed-t dispersion relations, they obtained the value $g_{\pi^\pm}^2/4\pi = 13.96 \pm 0.25$ (equivalent to $f_{\pi^\pm}^2 = 0.0771 \pm 0.0014$) [54]. From the analysis of NN elastic data between 210 and 800 MeV, Bugg and Machleidt [55] have deduced $g_{\pi^\pm}^2/4\pi =$

§ Using πNN Lagrangians as defined in the authoritative review [42], the relevant relationships between the pseudoscalar pion coupling constant, g_π, and the pseudovector one, f_π, are

$$\frac{g_{\pi^0 pp}^2}{4\pi} = \left(\frac{2M_p}{m_{\pi^\pm}}\right)^2 f_{\pi^0 pp}^2 = 180.773 f_{\pi^0 pp}^2 \tag{31}$$

and

$$\frac{g_{\pi^\pm}^2}{4\pi} = \left(\frac{M_p + M_n}{m_{\pi^\pm}}\right)^2 f_{\pi^\pm}^2 = 181.022 f_{\pi^\pm}^2 \ . \tag{32}$$

with $M_p = 938.272$ MeV the proton mass, $M_n = 939.566$ MeV the neutron mass, and $m_{\pi^\pm} = 139.570$ MeV the mass of the charged pion.

Table 3. Important coupling constants and the predictions for the deuteron and some *pp* phase shifts for five models discussed in the text.

	A	B	C	D	E	Empirical
Important coupling constants						
$g^2_{\bar{\pi}^0}/4\pi$	13.6	13.6	14.0	14.4	13.6	
$g^2_{\pi^\pm}/4\pi$	13.6	13.6	14.0	14.4	14.4	
κ_ρ	6.1	3.7	6.1	6.1	6.1	
The deuteron						
Q (fm^2)	0.270	0.278	0.276	0.282	0.278	0.276(2)[a]
η	0.0255	0.0261	0.0262	0.0268	0.0264	0.0256(4)[b]
A_S (fm$^{-1/2}$)	0.8845	0.8842	0.8845	0.8845	0.8847	0.8845(8)[c]
P_D (%)	4.83	5.60	5.11	5.38	5.20	–
$^3P_0$ *pp* phase shifts (deg)						
10 MeV	3.726	4.050	3.881	4.039	3.726	3.729(17)[d]
25 MeV	8.588	9.774	8.981	9.384	8.588	8.575(53)[d]
50 MeV	11.564	14.070	12.158	12.763	11.564	11.47(9)[d]

[a] Corrected for meson-exchange currents and relativity.
[b] Reference [62].
[c] Reference [63].
[d] Nijmegen *pp* multi-energy phase shift analysis [64].

13.69 ± 0.39 and $g^2_{\pi^0}/4\pi = 13.94 \pm 0.24$.

Thus, it may appear that recent determinations show a consistent trend towards a lower value for g_π with no indication for substantial charge dependence.

However, this is not true and for a comprehensive overview of recent determinations of the πNN coupling constant, see reference [56]. In particular, there is one determination that does not follow the above trend. Using a modified Chew extrapolation procedure, the Uppsala Neutron Research Group has deduced the charged-pion coupling constant from high precision *np* charge-exchange data at 162 MeV [57]. Their latest result is $g^2_{\pi^\pm}/4\pi = 14.52 \pm 0.26$ [58]. We note that the method used by the Uppsala Group is controversial [59, 60].

Since the pion plays a crucial role in the creation of the nuclear force, many NN observables are sensitive to the πNN coupling constant, g_π. We will discuss here the most prominent cases and their implications for an accurate value of g_π.

We will focus on the deuteron, NN analyzing powers A_y, and the singlet scattering length. Other NN observables with sensitivity to g_π are spin transfer coefficients. Concerning the latter and their implications for g_π, we refer the interested reader to references [55, 61].

3.1. The deuteron

The crucial deuteron observables to consider are the quadrupole moment, Q, and the asymptotic D/S state ratio, η. The sensitivity of both quantities to g_π is demonstrated in table 3. The calculations are based upon the CD-Bonn potential [65, 66]) which belongs to the new generation of high-precision NN potentials that fit the NN data below 350 MeV with a 'perfect' χ^2/datum of about one. The numbers in table 3 are an update of earlier calculations of this kind [67, 68] in which older NN potentials were applied. However, there are no substantial differences in the results as compared to the earlier investigations.

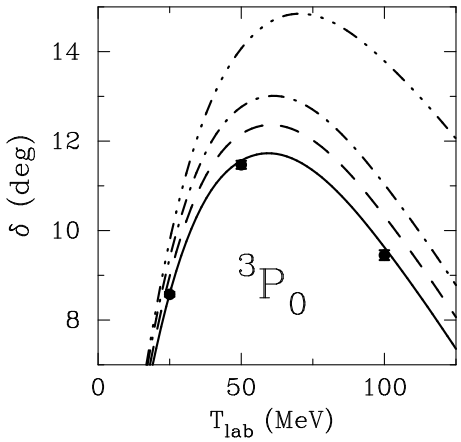

Figure 7. $^3P_0$ phase shifts of proton-proton scattering as predicted by Model A and E ($g^2_{\pi^0}/4\pi = 13.6$, solid line), B ($\kappa_\rho = 3.7$, dash-3dot), C ($g^2_{\pi^0}/4\pi = 14.0$, dashed), and D ($g^2_{\pi^0}/4\pi = 14.4$, dash-dot) ‖. The solid dots represent the Nijmegen *pp* multi-energy phase shift analysis [64].

For meaningful predictions, it is important that all deuteron models considered are realistic. This requires that besides the deuteron binding energy (that is accurately reproduced by all models of table 3) also other empirically well-known quantities are correctly predicted, like the deuteron radius, r_d, and the triplet effective range parameters, a_t and r_t. As it turns out, the latter quantities are closely related to the asymptotic S-state of the deuteron, A_S, which itself is not an observable. However, it has been shown [63] that for realistic values of r_d, a_t, and r_t, the asymptotic S-state of the deuteron comes out to be in the range $A_S = 0.8845 \pm 0.0008$ fm$^{-1/2}$. Thus, A_S plays the role of an important control number that tells us if a deuteron model is realistic or not. As can be seen from table 3, all our models pass the test.

Model A of table 3 uses the currently fashionable value for the πNN coupling constant $g^2_\pi/4\pi = 13.6$ which clearly underpredicts Q while η is predicted satisfactorily. One could now try to fix the problem with Q by using a weaker ρ-meson tensor-coupling to the nucleon, f_ρ. It is customary to state the strength of this coupling in terms of the tensor-to-vector ratio of the ρ coupling constants, $\kappa_\rho \equiv f_\rho/g_\rho$. Model A uses the 'large' value $\kappa_\rho = 6.1$ recommended by Hoehler and Pietarinen [69]. Alternatively, one may try the value implied by the vector-meson dominance model for the electromagnetic form factor of the nucleon [70] which is $\kappa_\rho = 3.7$. This is done in our Model B which shows the desired improvement of Q. However, a realistic model for the NN interaction must not only describe the deuteron but also NN scattering. As discussed in detail in reference [71], the small κ_ρ cannot reproduce the ϵ_1 mixing parameter correctly and, in addition, there are serious problems with the ^3P_J phase shifts, particularly, the $^3P_0$ (cf. lower part of table 3 and figure 7). Therefore, Model B is unrealistic and must be discarded.

The only parameters left to improve Q are g_π and the πNN vertex form-factor, $F_{\pi NN}$ (cf. equation 24, above). As for the ρ meson, $F_{\pi NN}$ is heavily constrained by NN phase parameters, particularly, ϵ_1. The accurate reproduction of ϵ_1 as determined in the Nijmegen *np* multi-energy phase shift analysis [64] essentially leaves no room

Table 4. χ^2/datum for the fit of the world *pp* A_y data below 350 MeV (subdivided into three energy ranges) using different values of the πNN coupling constant.

	Coupling constant $g^2_{\pi^0}/4\pi$			
Energy range (# of data)	13.2	13.6 A	14.0 C	14.4 D
0–17 MeV (45 data)	0.84	1.43	2.71	4.66
17–125 MeV (148 data)	1.05	1.06	1.54	2.45
125–350 MeV (624 data)	1.24	1.22	1.26	1.34

for variations of $F_{\pi NN}$ once the ρ meson parameters are fixed.

Thus, we are finally left with only one parameter to fix the Q problem, namely g_π. As it turns out, for relatively small changes of $g^2_\pi/4\pi$ there is a linear relationship, as demonstrated in table 3 by the predictions of Model A, C and D which use $g^2_\pi/4\pi = 13.6$, 14.0, and 14.4, respectively. Consistent with earlier studies [67, 68], one finds that $g^2_\pi/4\pi \geq 14.0$ is needed to correctly reproduce Q.

However, a pion coupling with $g^2_\pi/4\pi \geq 14.0$ creates problems for the $^3P_0$ phase shifts which are predicted too large at low energy (cf. lower part of table 3 and figure 7). Now, a one-boson-exchange (OBE) model for the NN interaction includes several parameters (about one dozen in total). One may therefore try to improve the $^3P_0$ by readjusting some of the other model parameters. The vector mesons (ρ and ω) have a strong impact on the $^3P_0$ (and the other P waves). However, due to their heavy masses, they are more effective at high energies than at low ones. Therefore, ρ and ω may produce large changes of the $^3P_0$ phase shifts in the range 200-300 MeV, with little improvement at low energies. The bottom line is that in spite of the large number of parameters in the model, there is no way to fix the $^3P_0$ phase shift at low energies. In this particular partial wave, the pion coupling constant is the only effective parameter, at energies below 100 MeV. The *pp* phase shifts of the Nijmegen analysis [64] as well as the *pp* phases produced by the VPI group [72] require $g^2_\pi/4\pi \leq 13.6$.

Notice that this finding is in clear contradiction to our conclusion from the deuteron Q.

There appears to be a way to resolve this problem. One may assume that the neutral pion, π^0, couples to the nucleon with a slightly different strength than the charged pions, $\pi^\pm$. This assumption of a charge-splitting of the πNN coupling constant is made in our Model E where we use $g^2_{\pi^0}/4\pi = 13.6$ and $g^2_{\pi^\pm}/4\pi = 14.4$. This combination reproduces the *pp* $^3P_0$ phase shifts at low energy well and creates a sufficiently large deuteron Q.

3.2. Analyzing powers

In our above considerations, some *pp* phase shifts played an important role. In principle, phase shifts are nothing else but an alternative representation of data. Thus, one may as well use the data directly. Since the days of Gammel and Thaler [4], it is well-known that the triplet P-wave phase shifts are fixed essentially by the NN analyzing powers, A_y. Therefore, we will now take a look at A_y data and compare them directly with model predictions.

In figure 8, we show high-precision *pp* A_y data at 9.85 MeV from Wisconsin [73]. The theoretical curves shown are obtained with $g^2_{\pi^0}/4\pi = 13.2$ (dotted), 13.6 (solid),

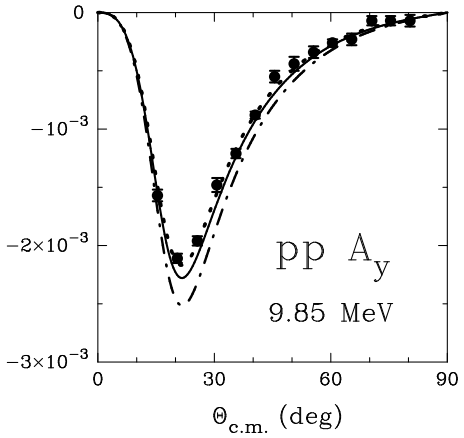

Figure 8. The proton-proton analyzing power A_y at 9.85 MeV. The theoretical curves are calculated with $g^2_{\pi^0}/4\pi = 13.2$ (dotted), 13.6 (solid, Model A), and 14.4 (dash-dot, Model D) and fit the data with a χ^2/datum of 0.98, 2.02, and 9.05, respectively. The solid dots represent the data taken at Wisconsin [73].

and 14.4 (dash-dot) and fit the data with a χ^2/datum of 0.98, 2.02, and 9.05, respectively. Clearly, a small coupling constant around 13.2 is favored. Since a single data set is not a firm basis, we have looked into all *pp* A_y data in the energy range 0–350 MeV. Our results are presented in table 4 where we give the χ^2/datum for the fit of the world *pp* A_y data below 350 MeV (subdivided into three energy ranges) for various choices of the neutral πNN coupling constant. It is seen that the *pp* A_y data at low energy, particularly in the energy range 0–17 MeV, are very sensitive to the πNN coupling constant. A value $g^2_{\pi^0}/4\pi \leq 13.6$ is clearly preferred, consistent with what we extracted from the single data set at 9.85 MeV as well as from the $^3P_0$ phase shifts.

Next, we look into the *np* A_y data. A single sample is shown in figure 9, the *np* A_y data at 12 MeV from TUNL [74]. Predictions are shown for Model A (solid line), D (dash-dot), and E (dash-triple-dot). The charge-splitting Model E fits the data best with a χ^2/datum of 1.00 (cf. table 5). We have also considered the entire *np* A_y data measured by the TUNL group [74] in the energy range 7.6–18.5 MeV (31 data) as well as the world *np* A_y data in the energy ranges 0–17 MeV (120 data). It is seen that there is some sensitivity to the πNN coupling constant in this energy range, while there is little sensitivity at energies above 17 MeV (cf. table 5).

Consistent with the trend seen in the 12 MeV data, the larger data sets below 17 MeV show a clear preference for a coupling constant around 14.4 if there is no charge splitting of g_π. This implies that without charge-splitting it is impossible to obtain an optimal fit of the *pp* and *np* A_y data. To achieve this best fit, charge-splitting is needed, like $g^2_{\pi^0}/4\pi = 13.6$ and $g^2_{\pi^\pm}/4\pi = 14.0$, as considered in column 5 of table 5. The drastic charge-splitting of Model E is not favored by the more comprehensive *np* A_y data sets.

The balance of the analysis of the *pp* and *np* A_y data then is: $g^2_{\pi^0}/4\pi \leq 13.6$ and $g^2_{\pi^\pm}/4\pi \geq 14.0$. Notice that this splitting is consistent with our conclusions from the deuteron. Thus, we have now some indications for charge-splitting of g_π from two

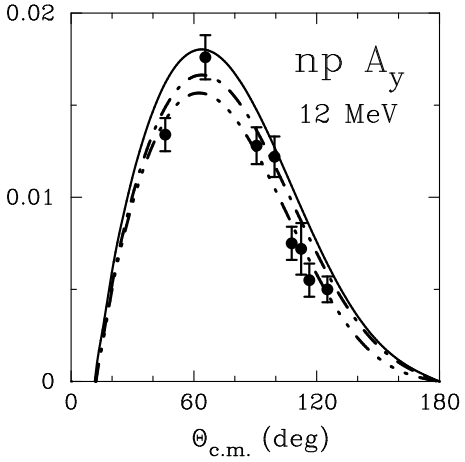

Figure 9. The neutron-proton analyzing power A_y at 12 MeV. The theoretical curves are calculated with $g^2_{\pi^0}/4\pi = g^2_{\pi^\pm}/4\pi = 13.6$ (solid line, Model A), $g^2_{\pi^0}/4\pi = g^2_{\pi^\pm}/4\pi = 14.4$ (dash-dot, Model D), and the charge-splitting $g^2_{\pi^0}/4\pi = 13.6$, $g^2_{\pi^\pm}/4\pi = 14.4$ (dash-3dot, Model E). The solid dots represent the data taken at TUNL [74].

very different observables, namely the deuteron quadrupole moment and np analyzing powers.

Therefore, it is worthwhile to look deeper into the issue of charge-splitting of the πNN coupling constant. Unfortunately, there are severe problems with any substantial charge-splitting—for two reasons. First, theoretical work [77] on isospin symmetry breaking of the πNN coupling constant based upon QCD sum rules comes up with a splitting of less than 0.5% for g^2_π and, thus, cannot explain the large charge splitting indicated above. Second, a problem occurs with the conventional explanation of the charge-dependence of the singlet scattering length, which we will explain now.

Table 5. χ^2/datum for the fit of various sets of np A_y data using different values for the πNN coupling constants.

	Coupling constants $g^2_{\pi^0}/4\pi$; $g^2_{\pi^\pm}/4\pi$				
Energy, data set (# of data)	13.6; 13.6 A	14.0; 14.0 C	14.4; 14.4 D	13.6; 14.0	13.6; 14.4 E
12 MeV [74] (9 data)	2.81	2.27	1.79	1.53	1.00
7.6–18.5 MeV [74] (31 data)	1.89	1.56	1.29	1.28	1.32
0–17 MeV world data (120)	1.17	1.03	0.94	0.99	1.19
17–50 MeV [75] (85 data)	1.16	1.12	1.14	1.18	1.18
17–125 MeV world data (416)	0.89	0.89	0.91	0.91	0.94

3.3. Charge-dependence of the singlet scattering length and charge-dependence of the pion coupling constant

Here, we are going to show in detail how charge-splitting of the πNN coupling constant affects the charge-dependence of the $^1S_0$ scattering length. It will turn out that the suggested charge-splitting of g_π causes a disaster for our established understanding of the charge-dependence of the singlet scattering length.

Our above considerations suggest charge-splitting of g_π, like

$$g^2_{\pi^0}/4\pi = 13.6\,, \tag{33}$$

$$g^2_{\pi^\pm}/4\pi = 14.4\,, \tag{34}$$

cf. Model E of table 3. We will now discuss how this charge-splitting of g_π affects Δa_{CIB} (more details can be found in the original paper reference [76]).

Accidentally, this splitting is—in relative terms—about the same as the pion-mass splitting; that is

$$\frac{g_{\pi^0}}{m_{\pi^0}} \approx \frac{g_{\pi^\pm}}{m_{\pi^\pm}}\,. \tag{35}$$

As discussed (cf. equations (25) and (30) and text below these equations), for zero momentum transfer, we have roughly for one-pion exachange

$$\mathrm{OPE} \sim \left(\frac{g_\pi}{m_\pi}\right)^2 \tag{36}$$

and for 2π exchange

$$\mathrm{TPE} \sim \left(\frac{g_\pi}{m_\pi}\right)^4\,, \tag{37}$$

which is not unexpected, anyhow. On the level of this qualitative discussion, we can then predict that any pionic charge-splitting satisfying equation (35) will create no CIB from pion exchanges. Consequently, a charge-splitting of g_π as given in equations (33) and (34) will wipe out our established explanation of CIB of the NN interaction.

In reference [76], accurate numerical calculations based upon the Bonn meson-exchange model for the NN interaction [24] have been conducted. The details of these calculations are spelled out in reference [36] where, however, no charge-splitting of g_π was considered. Assuming the g_π of equations (33) and (34), one obtains the Δa_{CIB} predictions given in the last column of table 6. It is seen that the results of an accurate calculation go even beyond what the qualitative estimate suggested: the conventional CIB prediction is not only reduced, it is reversed. This is easily understood if one recalls [cf. equations (25) and (30)] that the pion mass appears in the propagator $(m^2_\pi + \mathbf{k}^2)^{-1}$. Assuming an average $\mathbf{k}^2 \approx m^2_\pi$, the 7% charge splitting of m^2_π will lead to only about a 3% charge-dependent effect from the propagator. Thus, if a 6% charge-splitting of g^2_π is used, this will not only override the pion-mass effect, it will reverse it.

Based upon this argument and on the numerical results, one can then estimate that a charge-splitting of g^2_π of only about 3% (e. g., $g^2_{\pi^0}/4\pi = 13.6$ and $g^2_{\pi^\pm}/4\pi = 14.0$) would erase all predictions of CIB in the singlet scattering length derived from pion mass splitting.

Besides pion mass splitting, we do not know of any other essential mechanism to explain the charge-dependence of the singlet scattering length. Therefore, it is unlikely that this mechanism is annihilated by a charge-splitting of g_π. This may be taken as an indication that there is no significant charge splitting of the πNN coupling constant.

Table 6. Predictions for Δa_{CIB} in units of fm without and with the assumption of charge-dependence of g_π.

	No charge-dependence of g_π $g^2_{\pi^0}/4\pi = g^2_{\pi^\pm}/4\pi = 14.4$	**Charge-dependent g_π:** $g^2_{\pi^0}/4\pi = 13.6$ $g^2_{\pi^\pm}/4\pi = 14.4$
1π	3.24	–1.58
2π	0.36	–1.94
$\pi\rho, \pi\sigma, \pi\omega$	1.04	–0.97
Sum	4.64	–4.49
Empirical	5.64 ± 0.60	

3.4. Conclusions

Several NN observables can be identified that are very sensitive to the πNN coupling constant, g_π. They all carry the potential to determine g_π with high precision.

In particular, we have shown that the *pp* A_y data below 17 MeV are very sensitive to g_π and imply a value $g^2_\pi/4\pi \approx 13.2$. The *np* A_y data below 17 MeV show moderate sensitivity and the deuteron quadrupole moment shows great sensitivity to g_π; both *np* observables imply $g^2_\pi/4\pi \geq 14.0$.

The two different values may suggest a relatively large charge-splitting of g_π. However, a charge-splitting of this kind would completely destroy our established explanation of the charge-dependence of the singlet scattering length. Since this is unlikely to be true, we must discard the possibility of any substantial charge-splitting of g_π.

The conclusion then is that we are faced with real and substantial discrepancies between the values for g_π based upon different NN observables. The reason for this can only be that there are large, unknown systematic errors in the data and/or large uncertainties in the theoretical methods. Our homework for the future is to find these errors and eliminate them.

Another way to summarize the current confused situation is to state that, presently, any value between 13.2 and 14.4 is possible for $g^2_\pi/4\pi$ depending on which NN observable you pick. If we want to pin down the value more tightly, then we are faced with three possible scenarios:

- g_π is small, $g^2_\pi/4\pi \leq 13.6$:
  The deuteron η and *pp* scattering at low energies are described well; there are moderate problems with the *np* A_y data below 17 MeV. *The most serious problem is the deuteron Q.* Meson-exchange current contributions (MEC) and relativistic corrections for Q of 0.016 fm^2 or more would solve the problem. Present calculations predict about 0.010 fm^2 or less. A serious reinvestigation of this issue is called for.
- g_π is large, $g^2_\pi/4\pi \geq 14.0$:
  The deuteron Q is well reproduced, but η is predicted too large as compared to the most recent measurement by Rodning and Knutsen [62], $\eta = 0.0256(4)$. Note, however, that all earlier measurements of η came up with a larger value; for example, Borbely *et al.* [78] obtained $\eta = 0.0273(5)$. There are no objectively verifiable reasons why the latter value should be less reliable than the former one.

The deuteron η carries the potential of being the best observable to determine g_π (as pointed out repeatedly by Ericson [63, 79] in the 1980's); but the unsettled experimental situation spoils it all. The *np* A_y data at low energy are described well. *The most serious problem are the pp* A_y *data below 100 MeV.*

- g_π is 'in the middle', $13.6 \leq g_\pi^2/4\pi \leq 14.0$:
  we have all of the above problems, but in moderate form.

In conclusion, to arrive at an accurate value for g_π, there is a lot of homework to do—for theory and experiment.

4. Phase shift analysis

In spite of the large NN database available in the 1990's, conventional phase shift analyses are by no means perfect. For example, the phase shift solutions obtained by Bugg [80] or the VPI/GWU group [72] typically have a χ^2/datum of 1.3 or more, for the energy range 0–425 MeV. This may be due to inconsistencies in the data as well as deficiencies in the constraints applied in the analysis. In any case, it is a matter of fact that within the conventional phase shifts analysis, in which the lower partial waves are essentially unconstrained, a better fit cannot be achieved.

About two decades ago, the Nijmegen group embarked on a program to substantially improve NN phase shift analysis. To achieve their goal, the Nijmegen group took two decisive measures [64]. First, they 'pruned' the database; i.e., they scanned very critically the world NN database (all data in the energy range 0-350 MeV laboratory energy published in a regular physics journal between January 1955 and December 1992) and eliminated all data that had either an improbably high χ^2 (more than three standard deviations off) or an improbably low χ^2; of the 2078 world *pp* data below 350 MeV 1787 survived the scan, and of the 3446 *np* data 2514 survived. Second, they introduced sophisticated, semi-phenomenological model assumptions into the analysis. Namely, for each of the lower partial waves ($J \leq 4$) a different energy-dependent potential is adjusted to constrain the energy-dependent analysis. Phase shifts are obtained using these potentials in a Schroedinger equation. From these phase shifts the predictions for the observables are calculated including the χ^2 for the fit of the experimental data. This χ^2 is then minimized as a function of the parameters of the partial-wave potentials. Thus, strictly speaking, the Nijmegen analysis is a *potential analysis*; the final phase shifts are the ones predicted by the 'optimized' partial-wave potentials.

In the Nijmegen analysis, each partial-wave potential consists of a short- and a long-range part, with the separation line at $r = 1.4$ fm. The long-range potential V_L ($r > 1.4$ fm) is made up of an electromagnetic part V_{EM} and a nuclear part V_N:

$$V_L = V_{EM} + V_N \tag{38}$$

The electromagnetic interaction can be written as

$$V_{EM}(pp) = V_C + V_{VP} + V_{MM}(pp) \tag{39}$$

for proton-proton scattering and

$$V_{EM}(np) = V_{MM}(np) \tag{40}$$

for neutron-proton scattering, where V_C denotes an improved Coulomb potential (which takes into account the lowest-order relativistic corrections to the static

Coulomb potential and includes contributions of all two-photon exchange diagrams); V_{VP} is the vacuum polarization potential, and V_{MM} the magnetic moment interaction.

The nuclear long-range potential V_N consists of the local one-pion-exchange (OPE) tail $V_{1\pi}$ (the coupling constant g_π being one of the parameters used to minimize the χ^2) multiplied by a factor M/E and the tail of the heavy-boson-exchange (HBE) contributions of the Nijmegen78 potential [81] V_{HBE}, enhanced by a factor of 1.8 in singlet states; i. e.

$$V_N = \frac{M}{E} \times V_{1\pi}(g_\pi, m_\pi) + f(S) \times V_{HBE} \tag{41}$$

with $f(S = 0) = 1.8$ and $f(S = 1) = 1.0$, where S denotes the total spin of the two-nucleon system. The energy-dependent factor M/E (with $E = \sqrt{M^2 + q^2}$, $q^2 = MT_{lab}/2$) takes into account relativity in a 'minimal' way, damping the nonrelativistic OPE potential at higher energies.

As indicated, $V_{1\pi}$ depends on the πNN coupling constant g_π and the pion mass m_π, which gives rise to charge dependence. For pp scattering, the OPE potential is

$$V_{1\pi}^{pp} = V_{1\pi}(g_{\pi^0}, m_{\pi^0}) \tag{42}$$

with m_{π^0} the mass of the neutral pion. In np scattering, we have to distinguish between $T = 1$ and $T = 0$:

$$V_{1\pi}^{np}(T) = -V_{1\pi}(g_{\pi^0}, m_{\pi^0}) + (-1)^{T+1} 2V_{1\pi}(g_{\pi^\pm}, m_{\pi^\pm}) \tag{43}$$

The partial-wave short-range potentials ($r \leq 1.4$ fm) are energy-dependent square-wells (see figures 2 and 3 of reference [64]). The energy-dependence of the depth of the square-well is parametrized in terms of up to three parameters per partial wave. For the states with $J \leq 4$, there are a total of 39 such parameters (21 for pp and 18 for np) plus the pion-nucleon coupling constants (g_{π^0} and $g_{\pi^\pm}$).

In the Nijmegen np analysis, the $T = 1$ np phase shifts are calculated from the corresponding pp phase shifts (except in $^1S_0$ where an independent analysis is conducted) by applying corrections due to electromagnetic effects and charge dependence of OPE. Thus, the np analysis determines $^1S_0(np)$ and the $T = 0$ states, only.

In the combined Nijmegen pp and np analysis [64], the fit for 1787 pp data and 2514 np data below 350 MeV, available in 1993, results in the 'perfect' χ^2/datum = 0.99.

5. Recent additions to the NN database

The world NN data (below 350 MeV) published before December 1992 have been listed and analyzed carefully by the Nijmegen group in their papers about the Nijmegen phase shift analysis [47, 64]. Therefore, we will focus here on data published after 1992.

5.1. Proton-proton data

In the past decade, there has been a major breakthrough in the development of experimental methods for conducting hadron-hadron scattering experiments. In particular, the method of internal polarized gas targets applied in stored, cooled beams is now working perfectly in several hadron facilities, e. g., IUCF (Indiana, USA) and COSY (Jülich, Germany). Using this new technology, IUCF has produced a large

Table 7. After-1992 proton-proton data below 350 MeV. 'Error' refers to the normalization error. This table contains 1127 observables and 32 normalizations resulting in a total of 1159 data.

T_{lab} (MeV)	# observable	Error (%)	Institution(s)	Ref.
0.300–0.407	14 σ	None	Münster	[82]
25.68	8 D	1.3	Erlangen, Zürich, PSI	[83]
25.68	6 R	1.3	Erlangen, Zürich, PSI	[83]
25.68	2 A	1.3	Erlangen, Zürich, PSI	[83]
197.4	41 P	1.3	Wisconsin, IUCF	[84]
197.4	41 A_{xx}	2.5	Wisconsin, IUCF	[84]
197.4	41 A_{yy}	2.5	Wisconsin, IUCF	[84]
197.4	41 A_{xz}	2.5	Wisconsin, IUCF	[84]
197.4	39 A_{zz}	2.0	Wisconsin, IUCF	[85]
197.8	14 P	1.3	Wisconsin, IUCF	[86]
197.8	14 A_{xx}	2.4	Wisconsin, IUCF	[86]
197.8	14 A_{yy}	2.4	Wisconsin, IUCF	[86]
197.8	14 A_{xz}	2.4	Wisconsin, IUCF	[86]
197.8	10 D	None	IUCF	[61]
197.8	5 R	None	IUCF	[61]
197.8	5 R'	None	IUCF	[61]
197.8	5 A	None	IUCF	[61]
197.8	5 A'	None	IUCF	[61]
250.0	41 P	1.3	IUCF, Wisconsin	[87]
250.0	41 A_{xx}	2.5	IUCF, Wisconsin	[87]
250.0	41 A_{yy}	2.5	IUCF, Wisconsin	[87]
250.0	41 A_{xz}	2.5	IUCF, Wisconsin	[87]
280.0	41 P	1.3	IUCF, Wisconsin	[87]
280.0	41 A_{xx}	2.5	IUCF, Wisconsin	[87]
280.0	41 A_{yy}	2.5	IUCF, Wisconsin	[87]
280.0	41 A_{xz}	2.5	IUCF, Wisconsin	[87]
294.4	40 P	1.3	IUCF, Wisconsin	[87]
294.4	40 A_{xx}	2.5	IUCF, Wisconsin	[87]
294.4	40 A_{yy}	2.5	IUCF, Wisconsin	[87]
294.4	40 A_{xz}	2.5	IUCF, Wisconsin	[87]
310.0	40 P	1.3	IUCF, Wisconsin	[87]
310.0	40 A_{xx}	2.5	IUCF, Wisconsin	[87]
310.0	40 A_{yy}	2.5	IUCF, Wisconsin	[87]
310.0	40 A_{xz}	2.5	IUCF, Wisconsin	[87]
350.0	40 P	1.3	IUCF, Wisconsin	[87]
350.0	40 A_{xx}	2.5	IUCF, Wisconsin	[87]
350.0	40 A_{yy}	2.5	IUCF, Wisconsin	[87]
350.0	40 A_{xz}	2.5	IUCF, Wisconsin	[87]

number of *pp* spin correlation parameters of very high precision. In table 7, we list the new IUCF data together with other *pp* data below 350 MeV published between January 1993 and December 1999. The total number of after-1992 *pp* data is 1159, which should be compared to the number of *pp* data in the (Nijmegen) 1992 base, namely, 1787. Thus, the *pp* database has increased by about 2/3 since 1992. The importance of the new *pp* data is further enhanced by the fact that they are of much higher quality than the old ones.

The χ^2/datum produced by some recent phase shift analyses (PSA) and NN potentials in regard to the old and new databases are given in table 8. In this table, the '1992 database' is the Nijmegen database [47, 64] and the '1999 database' is the sum of the 1992 base and the after-1992 data.

Table 8. χ^2/datum for the NN data below 350 MeV applying some recent phase shift analyses (PSA) and NN potentials.

	VPI/GWU PSA [88]	Nijmegen 1993 PSA [64]	Argonne V_{18} pot. [89]	CD-Bonn pot. [66]
proton-proton data				
1992 *pp* database (1787 data)	1.28	1.00	1.10	1.00
After-1992 *pp* data (1145 data)[a]	**1.08**	**1.24**	**1.74**	**1.03**
1999 *pp* database (2932 data)[a]	1.21	1.09	1.35	1.01
neutron-proton data				
1992 *np* database (2514 data)	1.19	0.99	1.08	1.03
After-1992 *np* data (544 data)[b]	0.98[c]	0.99	1.02	0.99
1999 *np* database (3058 data)[b]	1.16[c]	0.99	1.07	1.02

[a]Without the 14 *pp* σ data of Ref. [82].
[b]Without after-1992 *np* σ data, except [92].
[c]Without the data of reference [91].

What stands out in table 8 are the rather large values for the χ^2/datum generated by the Nijmegen analysis and the Argonne potential for the the after-1992 *pp* data, which are essentially the new IUCF data. This fact is a clear indication that these new data provide a very critical test/constraint for any NN model. It further indicates that fitting the pre-1993 *pp* data does not nessarily imply a good fit of those IUCF data. On the other hand, fitting the new IUCF data does imply a good fit of the pre-1993 data. The conclusion from these two facts is that the new IUCF data provide information that was not contained in the old database. Or, in other words, the pre-1993 data were insufficient and still left too much lattitude for pinning down NN models. One thing in particular that we noticed is that the $^3P_1$ phase shifts above 100 MeV have to be lower than the values given in the Nijmegen analysis.

5.2. Neutron-proton data

Neutron-proton data published between January 1993 and December 1999 are listed in table 9. Particular attention deserve the TUNL data on $\Delta\sigma_L$ and $\Delta\sigma_T$ between 5 and 20 MeV [91] which made it possible to pin down the ϵ_1 mixing parameter with unprecedented precision.

Table 9 includes several new measurements of *np* differential cross sections (σ), with the largest sets produced by the Freiburg group [100] (871 data between 200 and 350 MeV), the Uppsala group [105, 98] (92 and 162 MeV, 109 data), and at Louvain-la-Neuve [96] (84 data between 29 and 73 MeV). In table 10 we show the χ^2/datum for the reproduction of these data sets by some recent PSA and NN potentials. One observes that none of the PSA and potentials can reproduce these data accurately. For comparison, table 10 includes the χ^2/datum for the *np* σ data by Bonner and coworkers [104] (652 data between 162 and 344 MeV, published in 1978) which are well reproduced. The large differences in the χ^2 implies that there are inconsistencies in the data. Since the PSA and potentials of table 10 were fitted to a database that includes the Bonner data but excludes the Freiburg data, one might suspect that this could be the explanation of the good χ^2 for the Bonner data and the bad one for Freiburg. Arndt has investigated this question [106] and found that this is not entirely true. When he excludes the Bonner data from the VPI/GWU analysis and uses the

Table 9. After-1992 neutron-proton data below 350 MeV. 'Error' refers to the normalization error.

T_{lab} (MeV)	# observable	Error (%)	Institution(s)	Ref.
3.65–11.6	9 $\Delta\sigma_T$	None	TUNL	[90]
4.98–19.7	6 $\Delta\sigma_L$	None	TUNL	[91]
4.98–17.1	5 $\Delta\sigma_T$	None	TUNL	[91]
14.11	6 σ	0.7	Tübingen	[92]
15.8	1 D_t	None	Bonn	[93]
16.2	1 $\Delta\sigma_T$	None	Prague	[94]
16.2	1 $\Delta\sigma_L$	None	Prague	[95]
29.0	6 σ	4.0	Louvain-la-Neuve	[96]
31.5	6 σ	4.0	Louvain-la-Neuve	[96]
34.5	6 σ	4.0	Louvain-la-Neuve	[96]
37.5	6 σ	4.0	Louvain-la-Neuve	[96]
41.0	6 σ	4.0	Louvain-la-Neuve	[96]
45.0	6 σ	4.0	Louvain-la-Neuve	[96]
49.0	6 σ	4.0	Louvain-la-Neuve	[96]
53.0	6 σ	4.0	Louvain-la-Neuve	[96]
58.5	6 σ	4.0	Louvain-la-Neuve	[96]
62.7	6 σ	4.0	Louvain-la-Neuve	[96]
67.7	15 σ	Float	Basel, PSI	[97]
67.7	6 σ	4.0	Louvain-la-Neuve	[96]
72.8	6 σ	4.0	Louvain-la-Neuve	[96]
162.0	54 σ	2.3	Uppsala	[98]
175.26	84 P	4.9[a]	TRIUMF	[99]
199.9	102 σ	3.0	Freiburg, PSI	[100]
203.15	100 P	4.7	TRIUMF	[99]
217.24	100 P	4.5	TRIUMF	[99]
219.8	104 σ	3.0	Freiburg, PSI	[100]
240.2	107 σ	3.0	Freiburg, PSI	[100]
260.0	8 R_t	3.0	PSI	[101]
260.0	8 A_t	3.0	PSI	[101]
260.0	3 A_t	3.0	PSI	[101]
260.0	8 D_t	3.0	PSI	[101]
260.0	3 D_t	3.0	PSI	[101]
260.0	8 P	2.0	PSI	[101]
260.0	3 P	2.0	PSI	[101]
261.00	88 P	4.1	TRIUMF	[99]
261.9	108 σ	3.0	Freiburg, PSI	[100]
280.0	109 σ	3.0	Freiburg, PSI	[100]
300.2	111 σ	2.6	Freiburg, PSI	[100]
312.0	24 P	4.0	SATURNE	[102]
312.0	11 A_{zz}	4.0	SATURNE	[103]
318.0	8 R_t	3.0	PSI	[101]
318.0	8 A_t	3.0	PSI	[101]
318.0	5 A_t	3.0	PSI	[101]
318.0	8 D_t	3.0	PSI	[101]
318.0	5 D_t	3.0	PSI	[101]
318.0	8 P	2.0	PSI	[101]
318.0	5 P	2.0	PSI	[101]
320.1	110 σ	2.1	Freiburg, PSI	[100]
340.0	112 σ	1.8	Freiburg, PSI	[100]

[a]This data set is floated in the χ^2 calculations of table 8 because all current phase shift analyses and *np* potentials predict a norm that is about 4 standard deviations off the experimental normalization error of 4.9%.

Table 10. χ^2/datum for various sets of neutron-proton differential cross section data below 350 MeV applying some recent phase shift analyses (PSA) and *np* potentials.

	VPI/GWU PSA [88]	Nijmegen 1993 PSA [64]	Argonne V_{18} potential [89]	CD-Bonn potential [66]
Bonner *et al.* [104], 652 data	1.18	1.08	1.20	1.10
Freiburg/PSI [100], 871 data	7.66	8.62	8.58	8.14
Uppsala [105, 98], 109 data	3.40	6.45	5.20	6.41
Louvain-la-Neuve [96], 84 data	3.22	3.15	3.12	3.17

Freiburg data instead, the latter can be reproduced with a χ^2/datum = 2.64 (the Bonner data produce χ^2/datum = 1.84 for this fit). Thus, the Freiburg data cannot be reproduced with the same accuracy as the Bonner data, even if one restricts the *np* σ data exclusively to Freiburg. This may be seen as an indication that there are inconsistencies within the Freiburg data. Certainly, the Bonner data and the Freiburg data are inconsistent with each other. Similar problems are observed with the Uppsala data, which are included in the VPI/GWU analysis and excluded from the Nijmegen PSA. The problems with the *np* differential cross sections deserve further systematic investigation.

6. The new high-precision NN potentials

In the 1990's, a focus has been on the quantitative aspect of NN potentials. Even the best NN models of the 1980's [24, 107] fit the NN data typically with a χ^2/datum ≈ 2 or more. This is still substantially above the perfect χ^2/datum ≈ 1. To put microscopic nuclear structure theory to a reliable test, one needs a perfect NN potential such that discrepancies in the predictions cannot be blamed on a bad fit of the NN data.

Based upon the Nijmegen analysis and the (pruned) Nijmegen database, new charge-dependent NN potentials were constructed in the early/mid 1990's. The groups involved and the names of their new creations are, in chronological order:

- Nijmegen group [108]: Nijm-I, Nijm-II, and Reid93 potentials.
- Argonne group [89]: V_{18} potential.
- Bonn group [65, 66]: CD-Bonn potential.

All these potentials have in common that they use about 45 parameters and fit the (pruned) 1992 Nijmegen data base with a χ^2/datum ≈ 1. However, as discussed in the previous section, since 1992 the *pp* database has substantially expanded and for the current database the χ^2/datum produced by some potentials is not so perfect anymore (cf. table 8).

6.1. Theoretical aspects

Concerning the theoretical basis of these potential, one could say that they are all—more or less—constructed 'in the spirit of meson theory' (e.g., all potentials include the one-pion-exchange contribution). However, there are considerable differences in the details leading to considerable off-shell differences among the potentials.

To explain these details and differences in a systematic way, let us first sketch the general scheme for the derivation of a meson-theoretic potential.

One starts from field-theoretic Lagrangians for meson-nucleon coupling, which are essentially fixed by symmetries. Typical examples for such Langrangians are:

$$\mathcal{L}_{ps} = -g_{ps}\bar{\psi}i\gamma^5\psi\varphi^{(ps)} \tag{44}$$

$$\mathcal{L}_{s} = -g_{s}\bar{\psi}\psi\varphi^{(s)} \tag{45}$$

$$\mathcal{L}_{v} = -g_{v}\bar{\psi}\gamma^{\mu}\psi\varphi^{(v)}_{\mu} - \frac{f_v}{4M}\bar{\psi}\sigma^{\mu\nu}\psi(\partial_\mu\varphi^{(v)}_{\nu} - \partial_\nu\varphi^{(v)}_{\mu}) \tag{46}$$

where ps, s, and v denote pseudoscalar, scalar, and vector couplings/fields, respectively.

The lowest order contributions to the nuclear force from the above Lagrangians are the second-order Feynman diagrams which, in the center-of-mass frame of the two interacting nucleons, produce the amplitude:

$$\mathcal{A}_\alpha(q',q) = \frac{\bar{u}_1(\mathbf{q}')\Gamma_1^{(\alpha)}u_1(\mathbf{q})P_\alpha\bar{u}_2(-\mathbf{q}')\Gamma_2^{(\alpha)}u_2(-\mathbf{q})}{(q'-q)^2 - m_\alpha^2}\ , \tag{47}$$

where $\Gamma_i^{(\alpha)}$ $(i=1,2)$ are vertices derived from the above Lagrangians, u_i are Dirac spinors representing the nucleons, and q and q' are the nucleon relative momenta in the initial and final states, respectively; P_α divided by the denominator is the meson propagator.

The simplest meson-exchange model for the nuclear force is the one-boson-exchange (OBE) potential [5] which sums over several second-order diagrams, each representing the single exchange of a different boson, α:

$$V(\mathbf{q}',\mathbf{q}) = \sqrt{\frac{M}{E'}}\sqrt{\frac{M}{E}}\sum_\alpha i\mathcal{A}_\alpha(\mathbf{q}',\mathbf{q})F_\alpha^2(\mathbf{q}',\mathbf{q})\ . \tag{48}$$

As customary, we include form factors, $F_\alpha(\mathbf{q}',\mathbf{q})$, applied to the meson-nucleon vertices, and a square-root factor $M/\sqrt{E'E}$ (with $E=\sqrt{M^2+\mathbf{q}^2}$ and $E'=\sqrt{M^2+\mathbf{q}'^2}$; M is the nucleon mass). The form factors regularize the amplitudes for large momenta (short distances) and account for the extended structure of nucleons in a phenomenological way. The square root factors make it possible to cast the unitarizing, relativistic, three-dimensional Blankenbecler-Sugar equation for the scattering amplitude (a reduced version of the four-dimensional Bethe-Salpeter equation) into a form which is identical to the (nonrelativistic) Lippmann-Schwinger equation (see reference [5] for details). Thus, equation (48) defines a relativistic potential which can be consistently applied in conventional, nonrelativistic nuclear structure.

Clearly, the Feynman amplitudes, equation (47), are in general nonlocal expressions; i. e., Fourier transforming them into configuration space will yield functions of r and r', the relative distances between the two in- and out-going nucleons, respectively. The square root factors create additional nonlocality.

While nonlocality appears quite plausible for heavy vector-meson exchange (corresponding to short distances), we have to stress here that even the one-pion-exchange (OPE) Feynman amplitude is nonlocal. This is important because the pion creates the dominant part of the nuclear tensor force which plays a crucial role in nuclear structure.

Applying $\Gamma^{(\pi)} = g_\pi\gamma_5$ in equation (47), yields the Feynman amplitude for one-pion exchange,

$$i\mathcal{A}_\pi(\mathbf{q}',\mathbf{q}) = -\frac{g_\pi^2}{4M^2}\frac{(E'+M)(E+M)}{(\mathbf{q}'-\mathbf{q})^2+m_\pi^2}\left(\frac{\sigma_{\mathbf{1}}\cdot\mathbf{q}'}{E'+M} - \frac{\sigma_{\mathbf{1}}\cdot\mathbf{q}}{E+M}\right)$$

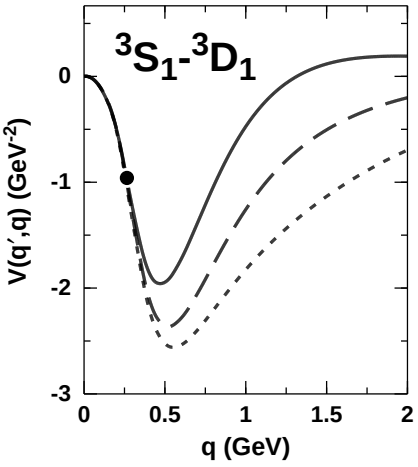

Figure 10. Half off-shell $^3S_1$–$^3D_1$ amplitude for the relativistic CD-Bonn potential (solid line), equation (48). The dashed curve is obtained when the local approximation, equation (51), is used for OPE, and the dotted curve results when this approximation is also used for one-ρ exchange. $q' = 265$ MeV/c.

$$\times \left(\frac{\sigma_2 \cdot \mathbf{q}'}{E' + M} - \frac{\sigma_2 \cdot \mathbf{q}}{E + M} \right) , \tag{49}$$

where m_π denotes the pion mass and isospin factors are suppressed. This is the original and correct result for OPE.

If one now introduces the drastic approximation,

$$E' \approx E \approx M , \tag{50}$$

then one obtains the momentum space representation of the *local* OPE,

$$V_{1\pi}^{(loc)}(\mathbf{k}) = -\frac{g_\pi^2}{4M^2} \frac{(\boldsymbol{\sigma_1} \cdot \mathbf{k})(\boldsymbol{\sigma_2} \cdot \mathbf{k})}{\mathbf{k}^2 + m_\pi^2} \tag{51}$$

with $\mathbf{k} = \mathbf{q}' - \mathbf{q}$. Notice that on-shell, i. e., for $|\mathbf{q}'| = |\mathbf{q}|$, $V_{1\pi}^{(loc)}$ equals $i\mathcal{A}_\pi$. Thus, the nonlocality affects the OPE potential off-shell.

Fourier transform of equation (51) yields the well-known local OPE potential in r-space,

$$V_{1\pi}^{(loc)}(\mathbf{r}) = \frac{g_\pi^2}{12\pi} \left(\frac{m_\pi}{2M} \right)^2 \left[\left(\frac{e^{-m_\pi r}}{r} - \frac{4\pi}{m_\pi^2} \delta^{(3)}(\mathbf{r}) \right) \boldsymbol{\sigma_1} \cdot \boldsymbol{\sigma_2} + \left(1 + \frac{3}{m_\pi r} + \frac{3}{(m_\pi r)^2} \right) \frac{e^{-m_\pi r}}{r} \boldsymbol{S_{12}} \right] . \tag{52}$$

Notice, however, that this 'well-established' local OPE potential is only an approximative representation of the correct OPE Feynman amplitude. A QED analog is the local Coulomb potential *versus* the full field-theoretic one-photon-exchange Feynman amplitude.

It is now of interest to know by how much the local approximation changes the original amplitude. This is demonstrated in figure 10, where the half off-shell $^3S_1$–$^3D_1$ potential, which can be produced only by tensor forces, is shown. The on-shell

Table 11. Modern high-precision NN potentials and their predictions for the two- and three-nucleon bound states.

	CD-Bonn [66]	Nijm-I [108]	Nijm-II [108]	Reid93 [108]	V_{18} [89]	NATURE
Character	nonlocal	mixed[a]	local	local	local	nonlocal
Deuteron properties:						
Quadr. moment (fm^2)	0.270	0.272	0.271	0.270	0.270	0.276(2)[b]
Asymptotic D/S state	0.0256	0.0253	0.0252	0.0251	0.0250	0.0256(4)[c]
D-state probab. (%)	4.85	5.66	5.64	5.70	5.76	–
Triton binding (MeV):						
nonrel. calculation	8.00	7.72	7.62	7.63	7.62	–
relativ. calculation	8.2	–	–	–	–	8.48

[a] Central force nonlocal, tensor force local.
[b] Corrected for meson-exchange currents and relativity.
[c] Reference [62].

momentum q' is held fixed at 265 MeV/c (equivalent to 150 MeV laboratory energy), while the off-shell momentum q runs from zero to 2000 MeV/c. The on-shell point ($q = 265$ MeV/c) is marked by a solid dot. The solid curve is the CD-Bonn potential which contains the full, nonlocal OPE amplitude equation (49). When the static/local approximation, equation (51), is made, the dashed curve is obtained. When this approximation is also used for the one-ρ exchange, the dotted curve results. It is clearly seen that the static/local approximation substantially increases the tensor force off-shell. Certainly, we are not dealing here with negligible effects, and the local approximation is obviously not a good one.

Even though the spirit of the new generation of potentials is more sophisticated, only the CD-Bonn potential uses the full, original, nonlocal Feynman amplitude for OPE, equation (49), while all other potentials still apply the local approximation, equations (51) and (52). As a consequence of this, the CD-Bonn potential has a weaker tensor force as compared to all other potentials. This is reflected in the predicted D-state probability of the deuteron, P_D, which is due to the nuclear tensor force. While CD-Bonn predicts $P_D = 4.85\%$, the other potentials yield $P_D = 5.7(1)\%$ (cf. table 11). These differences in the strength of the tensor force lead to considerable differences in nuclear structure predictions. An indication of this is given in table 11: The CD-Bonn potentials predicts 8.00 MeV for the triton binding energy, while the local potentials predict only 7.62 MeV. More discussion of this aspect can be found in references [5, 109].

The OPE contribution to the nuclear force essentially takes care of the long-range interaction and the tensor force. In addition to this, all models must describe the intermediate and short range interaction, for which very different approaches are taken. The CD-Bonn includes (besides the pion) the vector mesons $\rho(769)$ and $\omega(783)$, and two scalar-isoscalar bosons, σ, using the full, nonlocal Feynman amplitudes, equation (47), for their exchanges. Thus, all components of the CD-Bonn are nonlocal and the off-shell behavior is the original one that is determined from relativistic field theory.

The models Nijm-I and Nijm-II are based upon the Nijmegen78 potential [81]

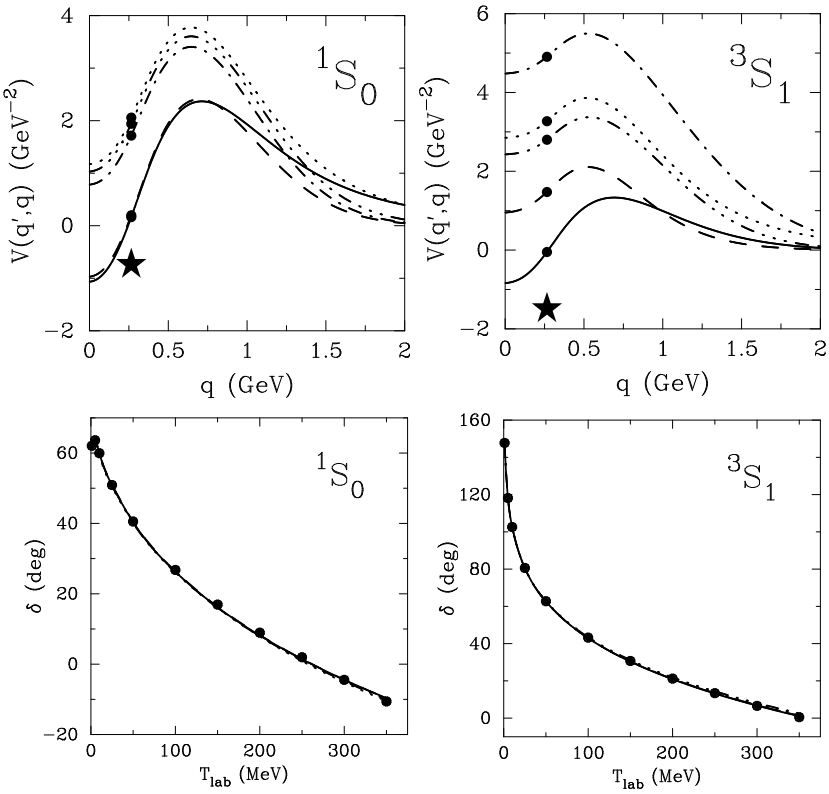

Figure 11. Upper part: Matrix elements $V(q', q)$ of the $^1S_0$ and $^3S_1$ potentials for the CD-Bonn (solid line), Nijm-I (dashed), Nijm-II (dash-dot), Argonne V_{18} (dash-triple-dot) and Reid93 (dotted) potentials. The diagonal matrix elements with $q' = q = 265$ MeV/c (equivalent to $T_{lab} = 150$ MeV) are marked by a solid dot. The corresponding matrix element of the scattering K-matrix is marked by the star. **Lower part:** Predictions for the np phase shifts in the $^1S_0$ and $^3S_1$ state by the five potentials. The five curves are essentially indistinguishable. The solid dots represent the Nijmegen multi-energy np analysis [64].

which is constructed from approximate OBE amplitudes. Whereas the Nijm-II uses the totally local approximations for all OBE contributions, the Nijm-I keeps some nonlocal terms in the central force component (but the Nijm-I tensor force is totally local). Nonlocalities in the central force have only a very moderate impact on nuclear structure as compared to nonlocalities in the tensor force. Thus, if for some reason one wants to keep only some of the original nonlocalities in the nuclear force and not all of them, then it would be more important to keep the tensor force nonlocalities.

The Reid93 [108] and Argonne V_{18} [89] potentials do not use meson-exchange for intermediate and short range; instead, a phenomenological parametrization is chosen. The Argonne V_{18} uses local functions of Woods-Saxon type, while Reid93 applies local Yukawas of multiples of the pion mass, similar to the original Reid potential of 1968 [110]. At very short distances, the potentials are regularized either by exponential (V_{18}, Nijm-I, Nijm-II) or by dipole (Reid93) form factors (which are all local functions).

In figure 11, the five high-precision potentials (in momentum space) and their phase shift predictions are shown, for the $^1S_0$ and $^3S_1$ states. While the phase shift predictions are indistinguishable, the potentials differ widely—due to the theoretical and mathematical differences discussed. Note that NN potentials differ the most in S-waves and converge with increasing L (where L denotes the total orbital angular momentum of the two-nucleon system).

6.2. Charge dependence

All new potentials are charge-dependent which is essential for obtaining a good χ^2 for the *pp* and *np* data. Thus, each potential comes in three variants: *pp*, *np*, and *nn*.

All potentials include the CIB effect from OPE. However, as discussed in section 2.2, pion mass splitting creates further CIB effects through the diagrams of 2π exchange and other two-boson exchange diagrams that involve pions. Another source of CIB is irreducible $\pi\gamma$ exchange. Recently, these contributions have been evaluated in the framework of chiral perturbation theory by van Kolck *et al.* [34]. In $L > 0$ states, the size of this contribution is typically the same as the CIB effect from TBE. Thus, TBE and $\pi\gamma$ create sizable CIB effects in states with $L > 0$. Therefore, a thoroughly constructed, modern, charge-dependent NN potential should include them. The NN potentials [108, 89] ignore these contributions while the latest CD-Bonn update [66] incorporates them.

A similar comment can be made about CSB. Most potentials include only the most trivial effects from nucleon mass splitting, namely the effect on the kinetic energy and on the OBE diagrams. However, as discussed in section 2.1.2, there are relatively large contributions from TBE that fully explain the CSB scattering length difference. Because of the outstanding importance of the CSB effect from TBE, it should be included in NN force models (and, therefore, it has been incorporated in the latest update of the CD-Bonn potential [66]). To have distinct *pp* and *nn* potentials is important for addressing several interesting issues in nuclear physics, like, the ^{3}H-^{3}He binding energy difference and the Nolen-Schiffer (NS) anomaly [111] regarding the energies of neighboring mirror nuclei. Potentials that do not include any CSB have no chance to ever explain these phenomena. Some potentials that include CSB focus on the $^1S_0$ state only, since this is where the most reliable empirical information is. However, even this is not good enough. A recent study [112] has shown that the CSB in partial waves with $L > 0$ as derived from the Bonn model is crucial for a quantitative explanation of the NS anomaly.

6.3. Extrapolating low-energy potentials towards higher energies

NN potentials designed for nuclear structure purposes are typically fitted to the NN scattering data up to pion production threshold or slightly beyond (e. g., 350 MeV). A very basic reason for this is that a real potential cannot describe the inelasticities of particle production. On the other hand, nuclear structure calculations are probably sensitive to the properties of a potential above 350 MeV. For example, the Brueckner G-matrix, which is a crucial quantity in many microscopic approaches to nuclear structure, is the solution of the integral equation,

$$G(\mathbf{q}', \mathbf{q}) = V(\mathbf{q}', \mathbf{q}) - \int d^3k V(\mathbf{q}', \mathbf{k}) \frac{M^\star Q}{k^2 - q^2} G(\mathbf{k}, \mathbf{q}) \tag{53}$$

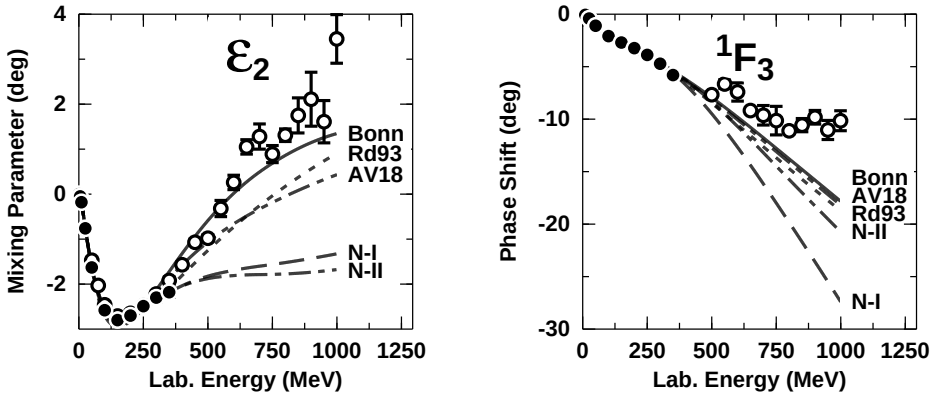

Figure 12. The ϵ_2 mixing parameter and the ${}^1F_3$ phase shift up to 1000 MeV lab. energy for various potentials as denoted (N-I and N-II refer to the Nijmegen potentials). Solid dots represent the Nijmegen PSA [64] and open circles the VPI/GWU analysis SM99 [72].

(where $M^\star$ denotes the effective nucleon mass and Q the Pauli projector). Notice that the potential V is involved in this equation for all momenta from zero to infinity, on- and off-shell. Now, it may very well be true that, as the momenta increase, their importance decreases (due to the short-range repulsion of the nuclear force and the associated short-range suppression of the nuclear wave function). However, it is also true that the impact of the potential does not suddenly drop to zero as soon as the momenta involved become larger than the equivalent of 350 MeV lab. energy. Thus, there are good arguments why NN potentials should extrapolate in a reasonable way towards higher energies.

We have investigated this issue and found good and bad news. The good news is that most potentials reproduce in most partial waves the NN phase shifts up to about 1000 MeV amazingly well. The bad news is that there are some singular cases where the reproduction of phase parameters for higher energies is disturbingly bad. The two most notorious cases are shown in figure 12. Above 350 MeV, the ϵ_2 mixing parameter is substantially underpredicted by both Nijmegen potentials (N-I and N-II). The reason for this is that, for ϵ_2, both potentials follow very closely the Nijmegen PSA [64] (solid dots in figure 12) up to 350 MeV. Thus, these potentials are faithfull extrapolations of the Nijmegen PSA to higher energies. Since this extrapolation is wrong, the suspicion is that the Nijmegen PSA has a wrong trend in the energy range 250-350 MeV. New data on *pp* spin transfer coefficients [61] in the energy range 300-500 MeV could resolve the issue.

A similar problem occurs in ${}^1F_3$ (figure 12). Here, the dashed curve (N-I) is the extrapolation of the Nijmegen PSA, indicating that the analysis may have the wrong trend in the energy range 200-350 MeV.

We note that, in the two channels discussed, the inelasticity has little impact on the phase parameters shown and would not fix the problems.

The moral is that one should not follow just one analysis, particularly, if that analysis is severely limited in its energy range. It is important to also keep the broad picture in mind.

7. The theory of nuclear forces: future directions

7.1. Critical summary of current status

During the past decade or so, the research on the NN interaction has proceeded essentially along two lines. There was the phenomenological line which has produced the high-precision, charge-dependent NN potentials [108, 89, 65, 66]. This was practical work, necessary to provide reliable input for exact few-body calculations and nuclear many-body theory.

The goal of the second line of research was to approach the problem on a more fundamental level. Since about 1980, we have seen many efforts to derive the nuclear force from the underlying theory of strong interactions, quantum chromodynamics (QCD). Due to its nonperturbative character in the low-energy regime, QCD cannot be solved exactly for the problem under consideration. Therefore, so-called QCD-related or QCD-inspired models have been developed, like, Skyrmion or Soliton models [113] and constituent quark cluster models. Among the quark models, one may distinguish between two types: the hybrid models [114] that include meson exchange and the quark delocalization and color screening models [115] that do not need (and do not include) meson exchange to create the intermediate-range attraction of the nuclear force. The success of all these efforts based upon QCD modelling is mixed. The qualitative features of the nuclear force are, in general, predicted correctly, but none of the models is sufficiently quantitative such that it would make sense to apply it in miscroscopic nuclear structure calculations.

In summary, one problem of the current status in the field is that quantitative models for the nuclear force have only a poor theoretical background, while theory based models yield only poor results. This discrepancy between theory and practice has become rather larger than smaller, in the course of the 1990s. Another problem is that the 'theory based models' are not strictly derived from QCD, they are modeled after QCD—often with handwoven arguments. Thus, one may argue that these models are not any better than the traditional meson-exchange models (that are nowadays perceived as phenomenology). The purpose of physics is to explain nature in fundamental terms. The two trends just discussed are moving us away from this aim, which is reason for serious concern.

Therefore, the main goal of future research on the nuclear force must be to overcome the above discrepancies. To achieve this goal, *we need a basic theory that is amenable to calculation and yields quantitative results.*

7.2. The effective field theory concept

In recent years, the concept of effective field theories (EFT) has drawn considerable attention in particle and nuclear physics [116, 117, 118]. The notion of *effective* field theories may suggest a difference to *fundamental* field theories. However, it is quite likely that all field theories (including those that we perceive presently as fundamental)

are effective in the sense that they are low-energy approximations to some 'higher' theory.

The basis of the EFT concept is the recognition of different energy scales in nature. Each energy level has its characteristic degrees of freedom. As the energy increases and smaller distances are probed, new degrees of freedom become relevant and must be included. Conversely, when the energy drops, some degrees of freedom become irrelevant and are frozen out.

To model the low-energy theory, one relies on a famous 'folk theorem' by Weinberg [119, 120] which states:

> If one writes down the most general possible Langrangian, including *all* terms consistent with assumed symmetry principles, and then calculates matrix elements with this Langrangian to any given order of perturbation theory, the result will simply be the most general possible S-matrix consistent with analyticity, perturbative unitarity, cluster decomposition, and the assumed symmetry principles.

The essential point of an effective field theory is that we are not allowed to make any assumption of simplicity about the Lagrangian and, consequently, we are not allowed to assume renormalizability. The Langrangian must include all possible terms, because this completeness guarantees that the effective theory is indeed the low-energy limit of the underlying theory. Now, this implies that we are faced with an infinite set of interactions. To make the theory managable, we need to organize a perturbation expansion. Then, up to a certain order in this expansion, the number of terms that contribute is finite and the theory will yield a well-defined result.

In strong interactions, the transition from the 'fundamental' to the effective level happens through a phase transition that takes place around $\Lambda_{QCD} \approx 1$ GeV via the spontaneous breaking of chiral symmetry which generates pseudoscalar Goldstone bosons. Therefore, at low energies ($E < \Lambda_{QCD}$), the relevant degrees of freedom are not quarks and gluons, but pseudoscalar mesons and other hadrons. Approximate chiral symmetry is reflected in the smallness of the masses of the pseudoscalar mesons. The effective theory that describes this scenario is known as chiral perturbation theory (χPT) [117, 121, 122].

If we believe in the basic ideas of EFT, then, at low energies, χPT is as fundamental as QCD at high energies. Moreover, due to its perturbative arrangement, χPT can be calculated: order by order. So, here we may have what we are asking for: *a basic theory that is amenable to calculation.* Therefore, χPT has the potential to overcome the discrepancy between theory and practice that has beset the theoretical research on the nuclear force for so many years.

7.3. Chiral perturbation theory and nuclear forces

The idea to derive nuclear forces from chiral effective Lagrangians is not new. A program of this kind was started some 10 years ago by Weinberg [123, 124], Ordóñez [125], and van Kolck [126, 127, 128] which produced the first chiral NN potential by Ordóñez, Ray, and van Kolck [129].

After the program was initiated, considerable activity ensued [130, 131, 132, 133, 134, 135, 136, 137, 138, 139, 140, 141]. For a recent review, see Ref. [142]. Even though all authors start from chiral effective Langrangians, there are differences in the details. There is, for example, the KSW scheme [135] in which the amplitude of interest is

calculated perturbatively. On the other hand, Weinberg proposed to use χPT for computing the NN potential which consists of irreducible diagrams. The S-matrix is then generated by the Schrödinger equation. The first comprehensive work using the Weinberg scheme was done by Ordóñez, Ray, and van Kolck [125, 126, 129] who applied time-ordered ('old-fashioned') perturbation theory to calculate the irreducible diagrams that define the potential. This potential posesses one unpleasant property, namely, it is energy dependent. One can avoid this problem by using the method of unitary transformations, a method that was pioneered by Okubo [143]. The Okubo tranformation is applied in the recent work by Epelbaum, Glöckle, and Meißner [144, 145] who construct chiral NN potentials in leading order (LO) of χPT, next-to-leading order (NLO), and next-to-next-to-leading order (NNLO). A systematic improvement in the ability of the model to reproduce the NN data is obseerved when stepping up the orders of the chiral expansion. The NNLO potential of Epelbaum *et al.* [145] describes the *np* phase shifts well up to about 100 MeV; above this energy there are discrepancies in some partial waves. This most recent chiral NN potential represents great progress as compared to earlier ones, however, for meaningfull applications in microscopic nuclear structure, futher quantitative improvements are necessary.

There is one particularly attractive aspect to the χPT approach in regard to those nuclear structure applications. If, in the traditional approach, one wants to reproduce, e. g., the experimental binding energies of the triton, the alpha particle or other nuclei, one complements the NN potential with a (phenomenological) three-nucleon force (3NF) [146]. Since different NN potentials leave different discrepancies to experiment (cf. table 11), the 3NF is adjusted from potential to potential. From a more fundamental point of view, this proceedure is very unsatisfactory, since it lacks any underlying systematics. However, within the framework of traditional meson theory, there is nothing else you can do, because there is no *a priori* connection between the off-shell NN potential and the existence of certain many-body forces.

In the framework of χPT, there is this connection from the outset. In each order of χPT, the two-nucleon force is well-defined on- and off-shell *and* it is also well-defined which 3NF terms occur in that order. At least that's how it should work 'in theory'. How it works out in practise remains to be seen.

8. NN scattering at intermediate and high energies

Even though the focus of this review is on the NN interaction at low energy (below pion production threshold), we like to give an indication of the exciting developments at higher energies to ensure that the reader gets an impression of the broader picture.

In the 1990's, a new experimental effort to measure *pp* scattering observables in the range 0.5 to 2.5 GeV of projectile energy was started. The experiments are conducted by the EDDA group [147, 148] at the cooled proton synchrotron (COSY) at Jülich, Germany, and use an internal target. The outstanding features of this new generation of experiments are high precision (high statistics) and small energy steps. Other experiments on NN observables at intermediate and high energies have been performed at SATURN II (Saclay, France) [149] and at facilities around the world; for a complete listing, see Ref. [150]. Moreover, there are the *pp* analyzing powers and spin correlation parameters, C_{NN}, that were measured up to lab. energies of 11.75 GeV by Alan Krisch and coworkers some 20 years ago at the Argonne Zero-Gradient-Synchrotron (ZGS) [151]. The latter data were never explained in a really

satisfatory way in spite of some efforts [152, 153]. During the past decade, theory has shown little interest in NN scattering at energies of 1-10 GeV and only a few papers can be cited [154, 155, 156, 157, 158, 159]. The reason for the neglect is probably that these energies are too high for traditional nuclear physicists and too low for high energy physicists; so, this range is the stepchild of both professions. But this is what makes this window particularly interesting: the energies are too high for χPT and too low for perturbative QCD. This fact implies that we have to find an appropriate phenomenology which calls for some phantasy and creativity. Relativistic, chiral meson models that include heavy mesons [like, $\rho(770)$ and $\omega(782)$] and nucleon resonances [like, the $\Delta(1232)$ isobar] are an obvious choice. In the language of EFT, these models can be justified on the basis of 'resonance saturation'. It will also be interesting to attempt matching of these high energy models with the χPT model discussed in the previous section.

It is well-known that relativistic meson models work satisfactorily up to about 1.2 GeV [160, 161, 162, 163, 164]; for a summary and critical discussion see section 7 of Ref. [5]. However, at energies above 1.5 GeV, characteristic problems occur, some of which are [165]:

- The predicted elastic NN cross sections are too large and grow with energy while experimentally they drop.
- The *pp* analyzing powers are predicted too large and for other spin observables (like, C_{NN}) even the sign is predicted wrong.

The first problem listed above is well-known since the late 1950's. The amplitude produced by vector-meson exchange is proportional to $s/(t-m_v^2)$ (with m_v the vector-meson mass and s,t the usual Mandelstam variables) which causes the elastic cross sections to rise with energy. Because of this problem, Regge theory [166, 167, 168, 169] was invented. Concerning the second problem listed above, we do not have a clue at this time. When the vector-meson contribution is 'phased out' such as to produce the correct elastic cross sections, then the problem with the analyzing powers persists, which is not what we expected. In any case, this energy region offers a wealth of good and unexplained data and a great diversity of potentially appropriate models, since we are truely at the intersection of nuclear and particle physics.

9. Summary and outlook

In the 1990's, we made major progress in our grasp on the nuclear force. NN data of unparalleled precision were produced, particularly at TUNL [90, 91], IUCF [61, 84, 85, 86, 87], and COSY [147, 148]. The art of NN phase shift analysis advanced substantially [64]. Based upon this empirical progress, NN potentials of unprecedented accuracy (χ^2/datum ≈ 1) were contructed [108, 89, 65, 66]. As a consequence of this, exact few-body calculations and miscroscopic nuclear many-body theory can now be based upon input that is more reliable than ever.

In spite of all this good news, there are also several questions concerning the NN interaction that remain open and future research should continue to address them. Among the more technical problems is the neutron-neutron scattering length where experiments are still in contradiction. There are problems with the determination of a precise value for the πNN coupling constant and, not unrelated, the huge and expensive database of neutron-proton differential cross sections [104, 105, 84, 100] is inconsistent.

On the theoretical side, we are still lacking a derivation of the nuclear force that is based upon theory (in the true sense of the word) and produces a quantitative NN potential. Moreover, our understanding of charge-dependence of the NN interaction is still incomplete, since we are not able to explain 25% of the charge-dependence of the $^1S_0$ scattering length.

Acknowledgments

This work was supported in part by the U.S. National Science Foundation under Grant No. PHY-9603097.

References

[1] Chadwick J 1932 *Proc. Roy. Soc. (London)* **A136** 692
[2] Rosenfeld L 1948 *Nuclear Forces* (Amsterdam: North-Holland)
Eder G 1965 *Kernkräfte* (Karlsruhe: Braun)
[3] Yukawa H 1935 *Proc. Phys. Math. Soc. Japan* **17** 48
[4] Gammel J L and Thaler R M 1957 *Phys. Rev.* **107** 291 and 1339
[5] Machleidt R 1989 *Adv. Nucl. Phys.* **19** 189
[6] Machleidt R and Li G Q 1994 *Phys. Rep.* **242** 5
[7] Slaus I, Akaishi Y and Tanaka H 1989 *Phys. Rep.* **173** 257
[8] Miller G A, Nefkens M K, and Slaus I 1990 *Phys. Rep.* **194** 1
[9] Miller G A and van Oers W H T 1995 *Symmetries and Fundamental Interactions in Nuclei* Haxton W C and Henley E M (ed) (Singapore: World Scientific) p 127
[10] Glashow D W *et al* 1986 *Radiation Effects* **94** 913
Glashow D W 1992 *LANL Report* LA-UR-92
[11] Howell C R *et al* 1998 *Phys. Lett.* B **444** 252
[12] González Trotter D E *et al* 1999 *Phys. Rev. Lett.* **83** 3788
[13] Gabioud B *et al* 1979 *Phys. Rev. Lett.* **42** 1508
Gabioud B *et al* 1981 *Phys. Lett.* B **103** 9
Gabioud B *et al* 1984 *Nucl. Phys.* A **420** 496
[14] Schori O *et al* 1987 *Phys. Rev.* C **35** 2252
[15] Slaus I *et al* 1982 *Phys. Rev. Lett.* **48** 993
[16] Glöckle W *et al* 1996 *Phys. Rep.* **274** 107
[17] Setze H R *et al* 1996 *Phys. Lett.* B **388** 229
[18] Tornow W *et al* 1996 *Few body systems* **21** 97
Tornow W 2000 Private communication
[19] Slobodrian R J *et al* 1984 *Phys. Lett.* B **135** 17
[20] Huhn V *et al* 2000 *Phys. Rev. Lett.* **85** 1190
Huhn V *et al* 2001 *Phys. Rev.* C **63** 014003
[21] Tippens W B *et al* 2000 *Phys. Rev.* C submitted
Batinic M *et al* 1997 *Proc. 15th Intl Conf on Few Body Problems in Physics* Book of Contributions p 419
A. Marusic 1997 Ph.D. thesis Univ of Zagreb
[22] Batinic M *et al* 1998 Physica Scripta **58** 15, and references therein
[23] Li G Q and Machleidt R 1998 *Phys. Rev.* C **58** 1393
[24] Machleidt R, Holinde K, and Elster C 1987 *Phys. Rep.* **149** 1
[25] Coon S A and Niskanen J A 1996 *Phys. Rev.* C **53** 1154
[26] Müther H, Polls A, and Machleidt R 1999 *Phys. Lett.* B **445** 259
[27] Goldman T, Henderson J A, and Thomas A W 1992 *Few-Body Systems* **12** 193
[28] Piekarewicz J and Williams A G 1993 *Phys. Rev.* C **47** 2462
[29] Krein G, Thomas A W, and Williams A G 1993 *Phys. Lett.* **B317** 293
[30] O'Connell H B, Pearce B C, Thomas A W, and Williams A G 1994 *Phys. Lett.* **B336** 1
[31] Coon S A, McKellar B H J, and Rawlinson A A 1997 *Intersections between Nuclear and Particle Physics* AIP Conf. Proc. **412** edited by T. W. Donelly (Woodbury, N.Y.) p 368
[32] O'Connell H B, Pearce B C, Thomas A W, and Williams A G 1997 *Prog. Part. Nucl. Phys.* **39** 201

[33] Coon S A and Scadron M D 2000 *Charge symmetry breaking via $\Delta I = 1$ group theory or by the u-d quark mass difference and direct photon exchange*, Proc. XXIII Symposium on Nuclear Physics, Oaxtepec, Mexico, January 2000, Revista Mexicana de Fisica, to be published
[34] van Kolck U, Rentmeester M C M, Friar J L, Goldman T, and de Swart J J 1998 *Phys. Rev. Lett.* **80** 4386
[35] Houk T L 1971 *Phys. Rev.* C **3** 1886
Dilg W 1975 *Phys. Rev.* C **11** 103
Koester L and Nistler W 1975 *Z. Physik* **A272** 189
Klarsfeld S, Martorell J, and Sprung D W L 1984 *J. Phys. G: Nucl. Phys.* **10** 165
[36] Li G Q and Machleidt R 1998 *Phys. Rev.* C **58** 3153
[37] Particle Data Group 2000 *Eur. Phys. J.* C **15** 1
[38] Ericson T E O and Miller G A 1983 *Phys. Lett.* **132B** 32
[39] Partovi M H and Lomon E L 1970 *Phys. Rev.* D **2** 1999
[40] Banerjee M K 1975 *Electromagnetic Interactions of Nucleons* University of Maryland Technical Report No. 75-050
[41] Chemtob M 1975 *Interaction Studies in Nuclei* edited by Jochim H and Ziegler B (Amsterdam: North-Holland) p 487
[42] Dumbrajs O *et al* 1983 *Nucl. Phys.* **B216** 277
[43] Bugg D V, Carter A A and Carter J R 1973 *Phys. Lett.* **B44** 278
[44] Koch R and Pietarinen E 1980 *Nucl. Phys.* **A336** 331
[45] Kroll P 1981 *Phenomenological Analysis of Nucleon-Nucleon Scattering*, Physics Data Vol. 22-1, H. Behrens and G. Ebel, eds. (Karlsruhe: Fachinformationszentrum)
[46] Bergervoet J R , van Campen P C, Rijken T A and de Swart J J 1987 *Phys. Rev. Lett.* **59** 2255
[47] Bergervoet J R, van Campen P C, Klomp R A M, de Kok J L, Rijken T A, Stoks V G J and de Swart J J 1990 *Phys. Rev.* C **41** 1435
[48] Arndt R A, Li Z J, Roper L D and Workman R L 1990 *Phys. Rev. Lett.* **65** 157
[49] Timmermans R G E 1997 *Few-Body Systems Suppl.* **9** 169
Timmermans R G E 1997 *πN Newsletter* **13** 80
Timmermans R G E 1998 *Nucl. Phys.* **A631** 343c
[50] Stoks V, Timmermans R and de Swart J J 1993 *Phys. Rev.* C **47** 512
[51] Arndt R A, Workman R L and Pavan M M 1994 *Phys. Rev.* C **49** 2729
[52] Arndt R A, Strakovsky I I and Workman R L 1994 *Phys. Rev.* C **50** 2731
[53] Arndt R A, Strakovsky I I and Workman R L 1995 *Phys. Rev.* C **52** 2246
[54] Markopoulou-Kalamara F G and Bugg D V 1993 *Phys. Lett.* **B318** 565
[55] Bugg D V and Machleidt R 1995 *Phys. Rev.* C **52** 1203
[56] *Proc. Workshop on Critical Issues in the Determination of the Pion-Nucleon Coupling Constant* (Uppsala, Sweden, June 1999) 2000 Physica Scripta **T87** 1
[57] Ericson T E O *et al* 1995 *Phys. Rev. Lett.* **75** 1046
[58] Rahm J *et al* 1998 *Phys. Rev.* C **57** 1077
[59] Rentmeester M C M, Klomp R A M and de Swart J J 1998 *Phys. Rev. Lett.* **81** 5253
Ericson T E O *et al* 1998 *Phys. Rev. Lett.* **81** 5254
[60] de Swart J J, Rentmeester M C M and Timmermans R G E 1998 *The Status of the Pion-Nucleon Coupling Constant* nucl-th/9802084
[61] Wissink S W *et al* 1999 *Phys. Rev. Lett.* **83** 4498
[62] Rodning N L and Knutsen L D 1990 *Phys. Rev.* C **41** 898
[63] Ericson T E O and Rosa-Clot M 1983 *Nucl. Phys.* **A405** 497
[64] Stoks V G J, Klomp R A M, Rentmeester M C M and de Swart J J 1993 *Phys. Rev.* C **48** 792
[65] Machleidt R, Sammarruca F and Song Y 1996 *Phys. Rev.* C **53** 1483
[66] Machleidt R 2000 *The high-precision, charge-dependent, Bonn nucleon-nucleon potential (CD-Bonn)* `arXiv:nucl-th/0006014`
[67] Machleidt R and Sammarruca F 1991 *Phys. Rev. Lett.* **66** 564
[68] Machleidt R and Li G Q 1993 *πN Newsletter* **9** 37
[69] Höhler G and Pietarinen E 1975 *Nucl. Phys.* **B95** 210
[70] Sakurai J J 1969 *Currents and Mesons* (Chicago: University of Chicago Press)
[71] Brown G E and Machleidt R 1994 *Phys. Rev.* C **50** 1731
[72] SAID, Scattering Analysis Interactive Dial-in facility by R. A. Arndt, I. I. Strakovsky, and R. L. Workman, Virginia Polytechnic Institute and State University, The George Washington University and Jefferson Lab.; for information on SAID and the VPI/GWU phase shift analysis, see reference [52]
[73] Barker M D *et al* 1982 *Phys. Rev. Lett.* **48** 918
Barker M D *et al* 1982 *Phys. Rev. Lett.* **49** 1056

[74] Weisel G J *et al* 1992 *Phys. Rev.* C **46** 1599
[75] Wilczynski K *et al* 1984 *Nucl. Phys.* **A425** 458
[76] Machleidt R and Banerjee M K 2000 *Few-Body Systems* **28** 139
[77] Hwang W Y P *et al* 1998 *Phys. Rev.* C **57** 61
[78] Borbely I, Grüebler W, Vuaridel B and König V 1989 *Nucl. Phys.* **A503** 349
[79] Ericson T E O 1984 *Comments Nucl. Part. Phys.* **13** 157
Ericson T E O and Rosa-Clot M 1985 *Ann. Rev. Nucl. Part. Sci.* **35** 271
Ericson T E O and Weise W 1988 *Pions and Nuclei* (Oxford: Clarendon Press)
[80] Bugg D V and Bryan R A 1992 *Nucl. Phys.* **A540** 449
[81] Nagels M M, Rijken T A and de Swart J J 1978 *Phys. Rev.* D **17** 768
[82] Dombrowski H, Khoukaz A and Santo R 1997 *Nucl. Phys.* **A619** 97
[83] Kretschmer W *et al* 1994 *Phys. Lett.* **B328** 5
[84] Rathmann R *et al* 1998 *Phys. Rev.* C **58** 658
[85] Lorentz B 1998 Ph.D. thesis University of Wisconsin-Madison
Lorentz B *et al* 2000 *Phys. Rev.* C **61** 054002
[86] Haeberli W *et al* 1997 *Phys. Rev.* C **55** 597
[87] v. Przewoski B *et al* 1998 *Phys. Rev.* C **58** 1897
[88] SAID (reference [72]) solution SP98
[89] Wiringa R B, Stoks V G J and Schiavilla R 1995 *Phys. Rev.* C **51** 38
[90] Wilburn W S, Gould C R, Haase D G, Huffman P R, Keith C D, Roberson N R and Tornow W 1995 *Phys. Rev.* C **52** 2351
[91] Raichle B W, Gould C R, Haase D G, Seely M L, Walston J R, Tornow W, Wilburn W S, Penttilä S I and Hoffman G H 1999 *Phys. Rev. Lett.* **83** 2711
Walston J R, Gould C R, Haase D G, Raichle B W, Seely M L, Tornow W, Wilburn W S, Penttilä S I and Hoffman G H 2001 *Phys. Rev.* C **63** 014004
[92] Buerkle W and Mertens G 1997 *Few-Body Systems* **22** 11
[93] Clotten P, Hempen P, Hofenbitzer K, Huhn V, Metschulat W, Schwindt M, Wätzold L, Weber C and von Witsch W 1998 *Phys. Rev.* C **58** 1325
[94] Brož J *et al* 1996 *Z. Physik* **A354** 401
[95] Brož J *et al* 1997 *Z. Physik* **A359** 23
[96] Benck S, Slypen I, Corcalciuc V and Meulders J P 1997 *Nucl. Phys.* **A615** 220
[97] Goetz J *et al* 1994 *Nucl. Phys.* **A574** 467
[98] Rahm J *et al* 1998 *Phys. Rev.* C **57** 1077
[99] Davis C A *et al* 1996 *Phys. Rev.* C **53** 2052
[100] Franz J, Rössle E, Schmitt H and Schmitt L 2000 *Physica Scripta* **T87** 14
Arndt R A 1999 Private communication
[101] Ahmidouch A *et al* 1998 *Eur. Phys. J.* **C2** 627
[102] Ball J *et al* 1993 *Nucl. Phys.* **A559** 489
[103] Ball J *et al* 1994 *Nucl. Phys.* **A574** 697
[104] Bonner B E *et al* 1978 Phys. Rev. Lett. **41** 1200
[105] Rönnqvist T *et al.* 1992 Phys. Rev. C **57** 1077
[106] Arndt R A 1999 Private communication
[107] Lacombe M, Loiseau B, Richard J M, Vinh Mau R, Côté J, Pirès P and de Tourreil R 1980 *Phys. Rev.* C **21** 861
[108] Stoks V G J, Klomp R A M, Terheggen C P F and de Swart J J 1994 *Phys. Rev.* C **49** 2950
[109] Machleidt R 1999 *Proc. Nuclear Structure 98*, Gatlinburg, Tennessee, 1998, AIP Conf. Proc. **481**, edited by C. Baktash (Woodbury, N.Y.: AIP) p 3
[110] Reid R V 1968 *Ann. Phys. (N.Y.)* **50** 411
[111] Nolen J A and Schiffer J P 1969 *Annu. Rev. Nucl. Sci.* **19** 471
[112] Müther H, Polls A and Machleidt R 1999 Phys. Lett. B **445** 259
[113] Jackson A, Jackson A D and Pasquier V 1985 *Nucl. Phys.* **A432** 567
Vinh Mau R, Lacombe M, Loiseau B, Cottingham W N and Lisboa P 1985 *Phys. Lett.* **150B** 259
Walhout T S and Wambach J 1992 *Int. J. Mod. Phys.* **E1** 665
Pepin S, Stancu F, Koepf W and Wilets L 1996 *Phys. Rev.* C **53** 1368
[114] Oka M and Yazaki K 1981 *Prog. Theor. Phys.* **66** 551 and 577
Faessler A, Fernandez F, Lübeck G, and Shimizu K 1982 *Phys. Lett.* B **112** 201
Faessler A, Fernandez F, Lübeck G, and Shimizu K 1983 *Nucl. Phys.* **A402** 555
Maltman K and Isgur N 1984 *Phys. Rev.* D **29** 952
Myhrer F and Wroldsen J 1988 *Rev. Mod. Phys.* **60** 629
Takeuchi S, Shimizu K and Yazaki K 1989 *Nucl. Phys.* **A504** 777

Fernandez F, Valcarce A, Straub U and Faessler A 1993 *J. Phys. G: Nucl. Part. Phys.* **19** 2013
Entem D R, Fernandez F and Valcarce A 2000 *Phys. Rev.* C **62** 034002
Shimizu K and Glozman L Y 2000 *Phys. Lett.* **B477** 59
[115] Wang F, Wu G H, Teng L J and Goldman T 1992 *Phys. Rev. Lett.* **69** 2901
Wu G H, Teng L J, Ping J L, Wang F and Goldman T 1996 *Phys. Rev.* C **53** 1161
Ping J L, Wang F and Goldman T 1999 *Nucl. Phys.* **A657** 95
Wu G H, Ping J L, Teng L J, Wang F and Goldman T 2000 *Nucl. Phys.* **A673** 279
[116] Georgi H 1993 *Annu. Rev. Nucl. Part. Sci.* **43** 209
[117] Ecker G 1995 *Prog. Part. Nucl. Phys.* **35** 1
[118] Kaplan D B 1995 *Effective Field Theories* `arXiv:nucl-th/9506035`
[119] Weinberg S 1979 *Physica* **96A** 327
[120] Weinberg S 1996 *What is Quantum Field Theory, and What Did We Think It Is?*, Talk presented at the conference "Historical Examination and Philosophical Reflections on the Foundations of Quantum Field Theory", Boston University, March 1996; in: *Boston 1996, Conceptual foundations and quantum field theory*, p. 241; `arXiv:hep-ph/9702027`
[121] Leutwyler H 1994 *Ann. Phys. (N.Y.)* **235** 165
[122] Bernard V, Kaiser N and Meißner U G 1995 *Int. J. Mod. Phys.* E **4** 193
[123] Weinberg S 1990 *Phys. Lett.* B **251** 288
Weinberg S 1991 *Nucl. Phys.* **B363** 3
[124] Weinberg S 1992 *Phys. Lett.* B **295** 114
[125] Ordonez C and van Kolck U 1992 *Phys. Lett.* B **291** 459
[126] van Kolck U 1993 Ph.D. thesis University of Texas, University of Washington Report DOE/ER/40427-13-N94
[127] van Kolck U 1994 *Phys. Rev.* C **49** 2932
[128] van Kolck U 1999 *Prog. Part. Nucl. Phys.* **43** 337
[129] Ordonez C, Ray L and van Kolck U 1994 *Phys. Rev. Lett.* **72** 1982
Ordonez C, Ray L and van Kolck U 1994 *Phys. Rev.* C **53** 2086
[130] Furnstahl R J, Serot B D and Tang H B 1997 *Nucl. Phys.* **A615** 441
Rusnak J J and Furnstahl R J 1997 *Nucl. Phys.* **A627** 495
Furnstahl R J, Rusnak J J and Serot B D 1997 `nucl-th/9709064`
Furnstahl R J, Steel J V and Tirfessa N 1999 `nucl-th/9910048`
[131] Celenza L S, Pantziris A and Shakin C M 1992 *Phys. Rev.* C **46** 2213
[132] Birse M C 1994 *Phys. Rev.* C **49** 2212
Richardson K G, Birse M C and Mc Govern J A 1997 `hep-ph/9708435`
Richardson K G 1999 Ph.D. thesis University of Manchester `hep-ph/0008118`
[133] da Rocha C A and Robilotta M R 1994 *Phys. Rev.* C **49** 1818
da Rocha C A and Robilotta M R 1995 *Phys. Rev.* C **52** 531
Robilotta M R and da Rocha C A 1997 *Nucl. Phys.* **A615** 391
Ballot J L, da Rocha C A and Robilotta M R 1998 *Phys. Rev.* C **57** 1574
[134] Park T S, Min D P and Rho M 1995 *Phys. Rev. Lett.* **74** 4153
Park T S, Min D P and Rho M 1996 *Nucl. Phys.* **A596** 515
Park T S, Min D P and Rho M 1999 *Nucl. Phys.* **A646** 83
Park T S, Kubodera K, Min D P and Rho M 1998 *Phys. Rev.* C **58** 637
[135] Kaplan D B, Savage M J and Wise M B 1996 *Nucl. Phys.* **B478** 629
Kaplan D B 1997 *Nucl. Phys.* **B494** 471
Savage M J 1997 *Phys. Rev.* C **55** 2185
Kaplan D B, Savage M J and Wise M B 1998 *Nucl. Phys.* **B534** 329
Kaplan D B, Savage M J and Wise M B 1998 *Phys. Lett.* **B424** 390
Kaplan D B, Savage M J and Wise M B 1999 *Phys. Rev.* C **59** 617
[136] Friar J L 1997 *Few-Body Systems* **22** 161
[137] Kaiser N, Brockmann R and Weise W 1997 *Nucl. Phys.* **A625** 758
Kaiser N, Gerstendörfer S and Weise W 1998 *Nucl. Phys.* **A637** 395
[138] Cohen T D 1997 *Phys. Rev.* C **55** 67
Phillips D R and Cohen T D 1997 *Phys. Lett.* **B390** 7
Phillips D R, Kao C W and Cohen T D 1997 *Phys. Rev.* C **56** 679
Beane S R, Cohen T D and Phillips D R 1998 *Nucl. Phys.* **A632** 445
[139] Fleming S, Mehen T and Stewart I W 1999 `nucl-th/9906056`, `nucl-th/9911001`
[140] Rupak G and Shoresh N 1999 `nucl-th/9902077`, `nucl-th/9906077`
[141] Bedaque P F, Hammer H W and van Kolck B 1998 *Phys. Rev.* C **58** 641
Bedaque P F, Hammer H W and van Kolck B 1999 *Nucl. Phys.* **A646** 444
[142] Beane S R, Bedaque P F, Haxton W C, Phillips D R and Savage M J 2000 `nucl-th/0008064`,

this is a chapter prepared for the *Handbook of QCD*
[143] Okubo S 1954 *Prog. Theor. Phys.* **12** 603
[144] Epelbaoum E, Glöckle W and Meißner U G 1998 *Nucl. Phys.* **A637** 107
[145] Epelbaum E, Glöckle W and Meißner U G 2000 *Nucl. Phys.* **A671** 295
[146] Nogga A, Kamada H and Glöckle W 2000 *Phys. Rev. Lett.* **85** 944
[147] Albers D *et al* 1997 *Phys. Rev. Lett.* **78** 1652
[148] Altmeier M *et al* 2000 *Phys. Rev. Lett.* **85** 1819
[149] Allgower C E *et al* 1999 *Phys. Rev.* C **60** 054001 and 054002
[150] Arndt R A *et al* 1997 *Phys. Rev.* C **56** 3005
Arndt R A *et al* 2000 *Phys. Rev.* C **62** 034005
[151] Fernow R C and Krisch A D 1981 *Ann. Rev. Nucl. Part. Sci.* **31** 107
Krisch A D 1985 *Lectures presented at the School on High Energy Spin Physics*, Lake Louise, Canada
[152] Brodsky S J and de Teramond G F 1988 *Phys. Rev. Lett.* **60** 1924
[153] Hoffmann J and Robson D 1990 *Phys. Rev.* C **42** 1225
[154] Neudatchin V G *et al* 1991 *Phys. Rev.* C **43** 2499
[155] LaFrance P, Lomon E L and Aw M 1993 *Improved coupled channels and R-matrix models: pp predictions to 1GeV* MIT preprint CTP#2133
[156] von Geram H V *et al* 1998 *Phys. Rev.* C **58** 1948
[157] Kochelev N I 1999 `hep-ph/9911480`
[158] Kharzeev D and Levin E 1999 `hep-ph/9912216`
[159] Gibbs W R and Loiseau B 2000 in preparation
[160] Kloet W M and Silbar R R 1980 *Nucl. Phys.* **A338** 281 and 317
Kloet W M and Silbar R R 1981 *Nucl. Phys.* **A364** 346
Dubach J, Kloet W M and Silbar R R 1982 *J. Phys. G* **8** 475
Dubach J, Kloet W M and Silbar R R 1982 *Nucl. Phys.* **A466** 573
[161] Lee T S H 1983 *Phys. Rev. Lett.* **50** 1571
Lee T S H 1984 *Phys. Rev.* C **29** 195
[162] van Faassen E E and Tjon J A 1984 *Phys. Rev.* C **30** 285
van Faassen E E and Tjon J A 1986 *Phys. Rev.* C **33** 2105
[163] ter Haar B and Malfliet R 1987 *Phys. Rep.* **149** 207
[164] Elster C, Holinde K, Schütte D and Machleidt R 1988 *Phys. Rev.* C **38** 1828
[165] Machleidt R 1999 *The nucleon-nucleon interaction at intermediate energies*, Proc. International Workshop on Intermediate Energy Spin Physics, Jülich, Germany, November 1998, F. Rathmann, W.T.H. van Oers, and C. Wilkin, eds. (Forschungszentrum Jülich, Jülich) p 169
[166] Collins P D B 1977 *An Introduction to Regge Theory and High Energy Physics* (Cambridge: Cambridge University Press)
[167] Perl M L 1974 *High Energy Hadron Physics* (New York: Wiley)
[168] *Regge Theory of Low p_t Hadronic Interactions* Caneschi L ed. 1989 (Amsterdam: North-Holland)
[169] Matthiae G 1994 *Rep. Prog. Phys.* **57** 743